

Probabilistic Forecasting of Climate Policy Uncertainty: The Role of Macro-financial Variables and Google Search Data

Donia Beshar¹, Anirban Sengupta², Tanujit Chakraborty^{1,3}

¹ SAFIR, Sorbonne University Abu Dhabi, United Arab Emirates.

² Indian Institute of Management, Bodhgaya, India.

³ Sorbonne Center for Artificial Intelligence, Sorbonne University, Paris, France.

Abstract

Accurately forecasting Climate Policy Uncertainty (CPU) is essential for designing climate strategies that balance economic growth with environmental objectives. Elevated CPU levels can delay regulatory implementation, hinder investment in green technologies, and amplify public resistance to policy reforms, particularly during periods of economic stress. Despite the growing literature documenting the economic relevance of CPU, forecasting its evolution and understanding the role of macro-financial drivers in shaping its fluctuations have not been explored. This study addresses this gap by presenting the first effort to forecast CPU and identify its key drivers. We employ various statistical tools to identify macro-financial exogenous drivers, alongside Google search data to capture early public attention to climate policy. Local projection impulse response analysis quantifies the dynamic effects of these variables, revealing that household financial vulnerability, housing market activity, business confidence, credit conditions, and financial market sentiment exert the most substantial impacts. These predictors are incorporated into a Bayesian Structural Time Series (BSTS) framework to produce probabilistic forecasts for both US and Global CPU indices. Extensive experiments and statistical validation demonstrate that BSTS with time-invariant regression coefficients achieves superior forecasting performance. We demonstrate that this performance stems from its variable selection mechanism, which identifies exogenous predictors that are empirically significant and theoretically grounded, as confirmed by the feature importance analysis. From a policy perspective, the findings underscore the importance of adaptive climate policies that remain effective across shifting economic conditions while supporting long-term environmental and growth objectives. By providing probabilistic forecasts of CPU, this study enables policymakers to conduct informed risk assessment, anticipate periods of heightened uncertainty, and design strategies that sustain climate objectives under varying economic conditions.

Keywords: Climate Policy Uncertainty, Macroeconomic and Financial Indicators, Bayesian Structural Time Series, Google Trends

1. Introduction

Since the early 19th century, industrialization has served as the principal catalyst of economic growth across both developed and developing nations; by the close of the 20th century, this role had increasingly shifted to the service sector, which emerged as the dominant force driving global economic expansion [43; 27]. However, this economic expansion has been accompanied by severe environmental degradation, particularly due to the emission of greenhouse gases (GHGs) such as carbon dioxide (CO_2) from industries and automobiles [90; 92; 30; 11]. In response, the Kyoto Protocol¹ was adopted on December 11, 1997 to mitigate this

¹For more details, refer to the official UNFCCC page on the Kyoto Protocol: <https://unfccc.int/kyoto-protocol>.

concern. The Kyoto Protocol required developed economies to reduce their emissions by an average of 5.2% below 1990 levels during the commitment period. However, the Paris Agreement², signed in 2015, expanded the responsibility to both the developing and developed economies ([35]). This broader commitment was also incorporated into the Sustainable Development Goals³ (SDGs), proposed by the United Nations in 2015, which call for global cooperation to balance environmental sustainability with economic progress. In particular, SDG 13 (Climate Action) and SDG 8 (Decent Work and Economic Growth) reflect the dual challenge of reducing emissions while sustaining development.

A central challenge in achieving sustainable growth lies in managing the uncertainty surrounding climate-related policy decisions. To quantify this uncertainty, Climate Policy Uncertainty (CPU) indices have been constructed for the United States (US) and globally [37; 65]. The US CPU index captures fluctuations in uncertainty associated with domestic legislative and regulatory developments, while the Global CPU index reflects uncertainty stemming from international climate policy developments and multilateral regulatory actions. Forecasting CPU is particularly relevant in light of the complex trade-offs that governments face between economic recovery and environmental commitments. Elevated levels of uncertainty lead to hesitation in long-term investments, especially in sectors sensitive to environmental regulation, such as energy, finance, and manufacturing [63; 98]. Such uncertainty can delay the transition toward cleaner technologies and hinder progress toward emission reduction goals [99; 85; 13]. Given the global need for substantial investments in low-carbon infrastructure, CPU represents a significant deterrent to both private and public sector decision-making [63; 13]. Moreover, CPU interacts with economic cycles and public perception. During recessions, policymakers often prioritize expansionary fiscal and monetary policies to stimulate consumption [44; 97], potentially sidelining climate mitigation policies [46; 51; 6; 93]. Public attention also shifts toward economic recovery, often viewing climate change as an obstacle [31; 38]. For example, during the post-COVID recovery, fiscal stimulus increased CO_2 emissions in China and MINT (Mexico, Indonesia, Nigeria, and Turkey) countries, as production rebounded from 2020 lows [1]. This trend is similar to the increase in CO_2 emissions in the US during 2022, making this trade-off a politically sensitive concern [29]. Therefore, understanding the extent to which the state of the economy drives changes in CPU can help policymakers design more resilient environmental regulations.

Economic indicators provide a broad picture of the state of the economy and underpin government and central bank policies. Gross domestic product (GDP) growth depends on industrial development, which results in employment and boosts national income, but at the expense of increased carbon emissions and threats to global warming due to reliance on non-renewable fossil-based sources of energy [75; 81]. This trade-off also extends to unemployment, highlighting the challenges of balancing development with climate goals [77]. In addition, interest rates and inflation play an essential role in the formation of climate change policies [3]. Expansionary monetary policies stimulate credit flows thereby increasing global liquidity and driving industrial activity, which further exacerbates global warming risks, whereas inflation discourages the adoption of cleaner, advanced technologies for industrial purposes. These interactions highlight how macroeconomic dynamics can amplify or mitigate environmental risks, making it essential to examine them within key economies that drive global trends.

The US, as the world's largest economy and the second-largest emitter of GHGs, plays a pivotal role in shaping global climate governance [69; 96]. Its economic cycles and financial market dynamics set the direction for international capital flows and policy responses [72]. Historical patterns reveal that GHG emissions in the US closely track economic activity. The CO_2 emissions fell sharply during the COVID-19 pandemic⁴. However, CO_2 emissions rebounded cumulatively by roughly 8% in 2022 relative to the 2020

²The Paris Agreement, adopted at COP21 in Paris, aimed to prevent the average global temperature from increasing by more than 2 degrees Celsius above preindustrial levels and to pursue efforts to limit the increase to 1.5 degrees Celsius. For more details, refer to the official UNFCCC page on the Paris Agreement: <https://unfccc.int/process-and-meetings/the-paris-agreement>.

³For more details, refer to the official UN page on the Sustainable Development Goals: <https://sdgs.un.org/goals>.

⁴US Environmental Protection Agency: <https://www.epa.gov/ghgemissions/sources-greenhouse-gas-emissions>.

pandemic low due to continued fossil fuel combustion [94]. Between 2020 and 2021, CO_2 emissions rose by 7%, followed by a more modest 1% increase between 2021 and 2022, reflecting the economic reopening and subsequent recovery. This pattern suggests that US business and financial cycles are deeply intertwined with climate outcomes and policy responses, underscoring the relevance of forecasting CPU. Supporting this view, [36] demonstrated that financial stress in the US significantly affects China’s CPU, implying that short-run macroeconomic conditions in the US can propagate CPU internationally. Meanwhile, the Environmental Kuznets Curve theory states that economic growth and human capital development encourage the adoption of cleaner technologies [60]. These considerations collectively motivate an investigation into how US macroeconomic and financial variables contribute to forecasting CPU.

Despite the growing recognition of CPU as a critical determinant of investment behavior, financial stability, and environmental outcomes, the existing literature has primarily examined its consequences rather than its predictability. Empirical studies have focused on the effects of CPU on volatility in renewable energy markets [98; 63], corporate investment decisions [66], and sovereign credit risk [74; 7; 100], consistently documenting that elevated CPU levels amplify financial and economic risks. This absence of research on the reverse relationship motivates our analysis. Consequently, this study constitutes the first systematic attempt to forecast CPU. Building on the above discussion regarding the interplay between economic activity, financial conditions, public perception, and policy uncertainty, we forecast CPU using a comprehensive set of 137 variables covering a broad range of macroeconomic and financial cycle indicators in the US, complemented by Google Trends data, which captures real-time shifts in public concern related to climate policy. Our analysis considers two US CPU indices to capture domestic dynamics and a Global CPU index to evaluate how US economic and financial conditions influence CPU globally.

Forecasting CPU presents substantial methodological challenges due to the high dimensionality of the covariate space and the presence of structural change and persistent volatility. Most standard econometric and machine learning approaches struggle in this setting, either due to overfitting or a loss of interpretability. To address these challenges, we employ a Bayesian Structural Time Series (BSTS) framework [89] to forecast CPU. BSTS is particularly well suited to this setting because it performs variable selection through its spike and slab prior on the regression coefficients, shrinking irrelevant covariates toward zero while retaining the most informative predictors. Moreover, BSTS is well-suited for policy-relevant forecasting as its credible intervals provide an explicit quantification of forecast uncertainty, enabling an assessment of the likelihood and magnitude of future CPU shocks. Such information is crucial for anticipating investment responses to regulatory uncertainty, guiding the timing and scale of climate policy interventions, and supporting more resilient policy design.

The suitability of BSTS for complex and uncertain forecasting environments is well established in the literature. In macroeconomics and finance, both univariate and multivariate extensions of BSTS have been successfully applied to forecasting stock portfolio returns, where the Bayesian framework effectively controls overfitting, captures cross-series dependence, and accommodates cyclical dynamics, yielding superior predictive performance relative to competing linear and multivariate time-series models [64]. Related work demonstrates the strengths of dynamic BSTS variants in energy and financial markets. In particular, dynamic BSTS models have been used to forecast crude oil prices using large information sets, enabling the identification of core economic drivers, structural turning points, and major regime shifts such as the global financial crisis [83]. In broader financial applications, BSTS has been employed to forecast stock prices in highly uncertain environments, where careful specification of state components has been shown to outperform traditional methods such as Holt-Winters and Seasonal Autoregressive Integrated Moving Average (SARIMA) [54]. Beyond financial markets, BSTS has also been applied in tourism economics to forecast international tourist arrivals under political instability and economic disruption, consistently delivering lower forecast errors than competing models and exhibiting robustness to regime changes and prolonged downturns [58; 5]. These studies highlight the ability of BSTS to integrate high-dimensional predictors, identify economically relevant variables, and remain robust to nonstationarity and evolving market conditions. These features make it particularly well-suited for forecasting CPU and providing policy-relevant insights into how

macroeconomic conditions, financial cycles, and public attention shape uncertainty surrounding climate policy decisions.

The main contribution of this paper is that, to the best of our knowledge, it represents the first attempt to forecast CPU. While prior research examines the effects of CPU on macroeconomic and financial markets, the question of whether CPU can be forecasted has remained unexplored. By reversing the prevailing direction of analysis in the literature, this study shifts the focus from the consequences of CPU to its underlying macro-financial predictors, thereby opening a new line of inquiry with direct relevance for environmental policy design and economic planning. Building on this main contribution, we introduce a macro-financial perspective to CPU forecasting by theoretically motivating how business cycle conditions and financial dynamics influence CPU and empirically validating these mechanisms. We identify a relevant subset of predictors using four complementary screening techniques and quantify the dynamic effect of unexpected changes in these variables on CPU via local projection impulse responses. We also incorporate Google search data to demonstrate that public attention to climate policy adds predictive power beyond traditional macro-financial variables. Finally, we empirically show that BSTS produces robust probabilistic forecasts and identifies economically meaningful predictors through analysis of the feature importance plot. Our analysis provides actionable insights into the dynamics of CPU, offering guidance for designing adaptive and resilient climate policies and supporting informed environmental and economic decision-making.

The remainder of the paper is structured as follows. Section 2 provides a literature review motivating forecasting with macroeconomic and financial cycle variables. Section 3 describes the datasets, summarizes their statistical properties, and highlights how CPU differs from general Economic Policy Uncertainty (EPU). Section 4 outlines the strategy for identifying CPU determinants and the criteria for incorporating Google search data. Section 5 introduces the BSTS framework. Section 6 presents the empirical findings, including statistical significance, insights from impulse response and feature importance analyses, and uncertainty quantification. Section 7 discusses the policy implications of the findings. Finally, Section 8 concludes the paper and highlights potential directions for future research.

2. Literature Review

CPU is closely intertwined with macroeconomic and financial conditions. For example, [6] and [93] reveal that CPU is linked to the business cycle conditions. During periods of economic expansion, governments are more likely to design and implement environmental policies addressing climate change and sustainability. Favorable fiscal balances, stronger employment, and higher corporate profitability increase the willingness of firms, households, and policymakers to comply with and support such regulations [71; 68]. By contrast, economic downturns weaken firms' commitment to invest in the technologies and infrastructure needed for regulatory compliance due to reduced profitability. Recessions also shift governmental priorities toward immediate economic stabilization, often relegating long-term environmental objectives to secondary importance [53; 78; 9; 55].

Macroeconomic indicators such as GDP, unemployment, and capacity utilization shape expectations regarding the financial and political feasibility of climate regulation. For instance, low-capacity utilization can prompt firms to defer green investments in order to hedge against the risk of the rollback of stringent environmental regulations under economic pressure from the government [47; 6]. Moreover, CPU is influenced by credit and financial market conditions. An increase in debt on balance sheets can demotivate the public and industrial sectors to comply with climate-related regulations [16; 12]. Macro-financial factors, including corporate bond yields, credit spreads, bank lending, and system-wide leverage, affect CPU because the implementation of climate policy requires high capital investments, tight credit markets, and rising interest rates, which can have an adverse impact on the adoption of climate policies. Investment in renewable energy depends on the availability of credit and the cost of capital. Tighter financial conditions, such as an increase

in interest rates and term spreads, increase the cost of new investments required for decarbonization and heighten uncertainty about the scale and persistence of regulatory commitments [14; 62]. Furthermore, [17] and [22] demonstrate that transition risk and expectations regarding environmental policy are embedded in equity and credit markets. This implies that fluctuations in financial conditions directly shape perceptions of future regulatory regimes.

Energy and commodity prices are another structural determinant of CPU. Increases in oil prices raise production and transportation costs, as well as household energy expenditures, leading to higher inflation. This effect heightens the short-term economic cost of climate policies and can reduce public willingness to bear transition costs. [45; 57], and [18] underline such interaction between energy prices, inflation, and policy uncertainty. Asset market valuations and volatility further influence CPU by reflecting forward-looking expectations about the profitability of carbon-intensive versus green technologies and the credibility of regulatory commitments. Risk aversion tends to increase during periods of high market volatility, leading to policy ambiguity and uncertainty regarding long-term climate strategies [15; 10; 82; 65]. Overall, the literature supports our approach of forecasting CPU using macroeconomic and financial variables, as these factors capture key channels through which economic and financial conditions influence CPU. We further examine these channels empirically via impulse response analysis in Section 6.6 to quantify how fluctuations in these variables dynamically affect CPU.

3. Data Overview and Descriptive Analysis

This study aims to forecast three monthly CPU indices. Although CPU is conceptually related to the broader Economic Policy Uncertainty (EPU) index [10], the two indices differ fundamentally in scope and implications. While EPU captures uncertainty surrounding general macroeconomic, fiscal, and monetary policy decisions, CPU specifically reflects uncertainty tied to environmental and climate policies. Evidence shows that CPU provides distinct predictive insights for green energy markets [48], corporate investment [49], green innovation [8], and the adoption of climate-aligned technologies [26]. This evidence highlights CPU as a more relevant indicator for assessing uncertainty arising from environmental governance both domestically and globally.

To capture these dynamics, we consider a *primary US CPU index* [37] that captures monthly fluctuations in climate policy as reported by eight major newspapers: *Wall Street Journal*, *Boston Globe*, *Los Angeles Times*, *Chicago Tribune*, *New York Times*, *Tampa Bay Times*, *Miami Herald*, and *USA Today*. To ensure robustness across construction and coverage, we include an *alternative US CPU index* and a *Global CPU index* [65]. The alternative US index is derived from a comparable news-based textual analysis but differs in sources and aggregation, providing an independent measure of CPU in the US. The Global CPU index is constructed using news articles from major newspapers across twelve countries: China, Japan, Korea, India, South Africa, the US, Canada, Brazil, the United Kingdom, France, Germany, and Australia. Following a keyword-based textual analysis framework, CPU is first measured at the country level and then aggregated into a global index using purchasing power parity (PPP)-adjusted GDP weights. This weighting scheme ensures that larger economies exert proportionate influence on the global measure. The resulting index captures the dynamics of CPU associated with major international climate events and global regulatory developments. Alongside the CPU indices, we compiled a comprehensive set of macroeconomic and financial cycle indicators capturing aggregate economic activity, credit markets, asset prices, labor markets, and housing dynamics. This setup allows us to assess whether US-based macro-financial predictors remain informative for global CPU. To incorporate behavioral and public sentiment, we also include climate-related search terms derived from Google Trends. The resulting integrated dataset enables analysis of how macro-financial conditions and public attention jointly influence CPU.

The primary US CPU index used in this analysis is a monthly series running from April 1987 to June

Table 1: Financial cycle variables, where x_t denotes the respective time series and x_{t-k} denotes the respective time series with k lags. Source details adapted from [73].

Variable Name	Label	Source	Transformation	Mathematical Construction
Business Confidence Index	bci	OECD	x_t	Normalized index measuring business sentiment
Composite Leading Indicator	cli	OECD	x_t	Amplitude adjusted leading indicator of economic activity
Real S&P 500 Index Growth	sp500	Shiller	$\ln(x_{t-1}) - \ln(x_{t-4})$	3-month lagged quarterly log growth of S&P500
Cyclically Adjusted Price Earnings Ratio	cape	Shiller	$\ln(x_t)$	Ratio of current share price to 10-year inflation adjusted earnings
Real Credit Growth	cred	FRED	$\ln(x_{t-1}) - \ln(x_{t-4})$	3-month lagged quarterly log growth of real credit
Credit-to-GDP Ratio	cred_gdp	BIS	x_t	Ratio of credit to private non-financial sector to nominal GDP
Real House Price Growth	hpi	Shiller	$\ln(x_{t-1}) - \ln(x_{t-4})$	3-month lagged quarterly log growth of house prices
Cyclically Adjusted Price-to-Rent Ratio	capr	FRED	$\ln(x_t)$	Ratio of house price index to rent price index
Real Mortgage Debt Growth	mortg	FRED	$\ln(x_{t-1}) - \ln(x_{t-4})$	3-month lagged quarterly log growth of mortgage debt
Household Mortgage-to-Income Ratio	mortg_inc	FRED	x_t	Ratio of household mortgage debt liability to personal income
Residential Investment-to-GDP Ratio	prfi_gdp	FRED	x_t	Ratio of private residential fixed investment to nominal GDP
Interest Payments-to-Income Ratio	pip_inc	FRED	x_t	Ratio of personal interest payments to personal income
National Financial Conditions Index	nfcf	FRED	x_t	Chicago Fed National Financial Conditions Index

2023, comprising 435 observations, and is sourced from the Economic Policy Uncertainty website (https://www.policyuncertainty.com/climate_uncertainty.html). The alternative US and Global CPU indices are monthly series spanning January 2000 to June 2023, with 282 observations, and are obtained from the China Energy and Environmental Policy Research Center Network website (<http://www.cnefn.com>). We also investigated 137 variables predominantly from the FRED-MD dataset [67] depicting the US macroeconomic and financial cycle variables. All of these variables are listed and briefly described in Table A.10 in Appendix A.5. These variables include key macroeconomic indicators such as GDP, inflation, unemployment rates, labor market metrics, credit conditions, and financial indices, providing a comprehensive view of the US economy. [67] proposed presenting this large macroeconomic dataset quarterly. Later, a monthly version of this dataset was introduced. To ensure transparency and reproducibility, further details about the transformations applied to this data are provided in [67] and summarized in Table 1. This dataset has been earlier used to forecast economic policy, commodity risk premiums, and US GDP in [23; 84]; and [73].

The summary statistics and global characteristics of the training samples for the primary US, alternative US, and Global CPU indices are reported in Tables 2 and 3, respectively. The training period for the primary US CPU index spans April 1987 to June 2021, while the training samples of the alternative US and Global CPU indices run from January 2000 to June 2021. Table 2 presents key descriptive measures, including the coefficient of variation (CoV), which measures variability relative to the mean, and entropy, which captures the complexity and uncertainty inherent in the distribution of the CPU index. Across all three indices,

the CoV values indicate substantial variability relative to the mean, with the alternative US CPU index exhibiting the highest relative dispersion. Table 3 reports key time series properties including distributional shape (skewness and kurtosis), nonlinearity, seasonality, and long-range dependence [50]. All three CPU series are right-skewed, with the primary US CPU index exhibiting pronounced asymmetry and heavier tails, while the alternative US and Global CPU indices display more moderate skewness and kurtosis. These distributional characteristics indicate a non-negligible probability of elevated CPU episodes across indices, albeit with varying magnitudes. The time series plots portrayed in Table 4 reveal significant variability in CPU, marked by periods of intensified uncertainty in policy direction. The plots depict a clear upward trend across indices, reflecting an increase in climate-related policies over time. While the trend is generally stable, noticeable spikes do correspond to major world events or changes in climate policy. Linearity tests based on Tsay’s and Keenan’s one-degree procedures indicate nonlinear dynamics for the primary US and Global CPU indices, whereas the alternative US CPU index exhibits predominantly linear behavior. Seasonality is detected exclusively in the primary US CPU index using the Ollech and Weibel test, while all three series are found to be nonstationary according to the Kwiatkowski-Phillips-Schmidt-Shin (KPSS) test. Finally, the Hurst exponent provides evidence of the presence of long-range dependence in all three CPU series. This characteristic is further examined through autocorrelation analysis. The autocorrelation function (ACF) and partial autocorrelation function (PACF) plots in Table 4 reveal a pronounced autocorrelation structure, indicating that past values of the CPU series exert a persistent influence on future values across multiple lags. Given the presence of such properties, it is essential to adopt a modeling framework that explicitly accounts for structural components.

Table 2: Summary statistics of the training samples for the three CPU indices.

CPU Index	Min Value	Q1	Median	Mean	Q2	Max Value	CoV	Entropy
Primary (US)	28.162	63.563	84.166	94.876	108.046	346.612	49.777	6.019
Alternative (US)	0.120	0.881	1.425	1.485	1.945	4.114	56.953	5.547
Global	28.500	67.591	86.115	90.895	109.719	215.088	37.603	5.553

Table 3: Statistical characteristics of the training samples for the three CPU indices.

CPU Index	Skewness	Kurtosis	Linearity	Seasonality	Stationarity	Long Range Dependence
Primary (US)	1.863	4.531	Nonlinear	Seasonal	Nonstationary	0.780
Alternative (US)	0.664	0.376	Linear	Nonseasonal	Nonstationary	0.699
Global	0.849	0.871	Nonlinear	Nonseasonal	Nonstationary	0.759

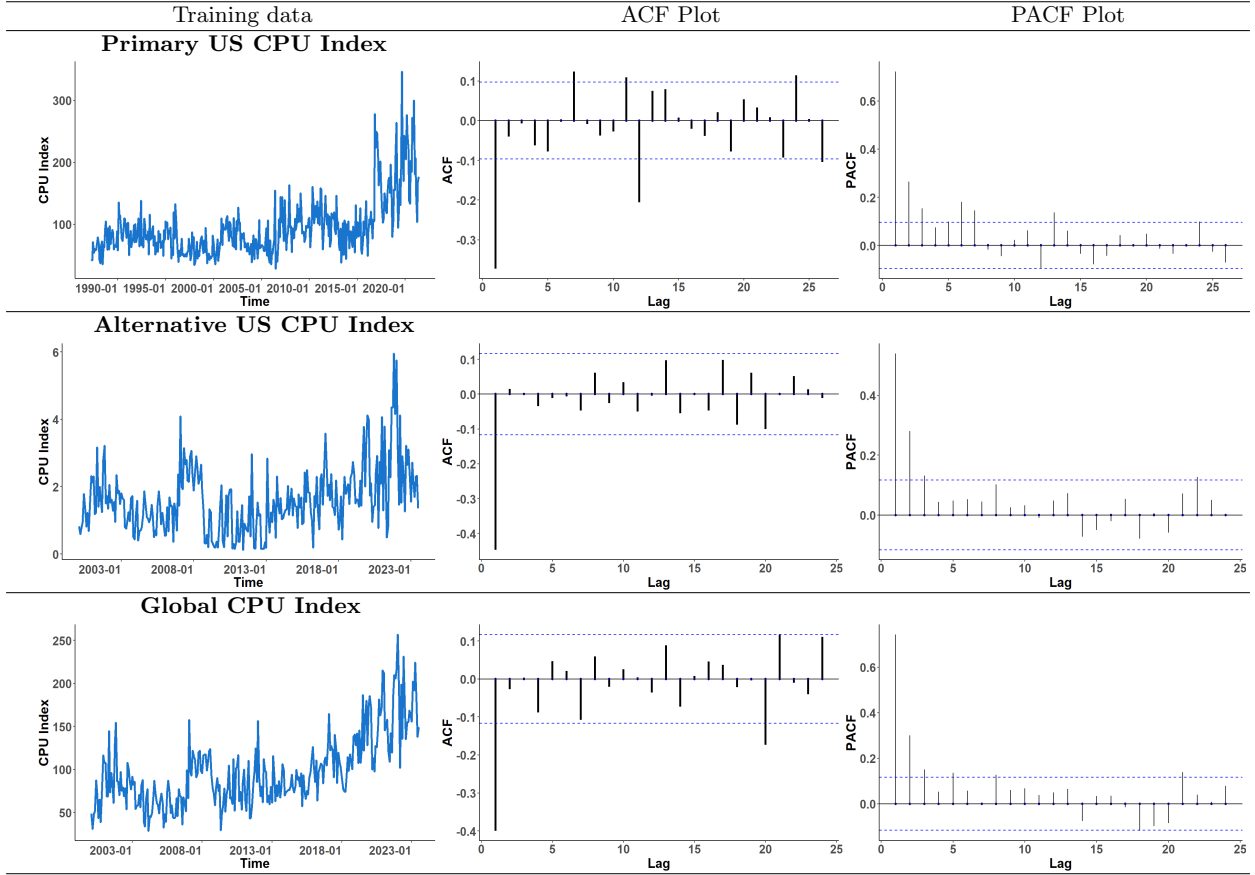
4. Identifying the Predictors of the CPU Index

This section examines the association between macroeconomic, financial, and information-based factors with the CPU index. We begin by describing the empirical screening frameworks used to identify relevant predictors (Section 4.1), followed by an outline of the theoretical justification for the selected variables (Section 4.2). Finally, we discuss the role of information variables derived from Google search data (Section 4.3).

4.1. Variable Screening and Predictor Selection

This section describes the multi-stage screening framework used to identify predictors that are empirically associated with movements in the CPU index. The objective is to reduce the dimensionality of a large initial set of macroeconomic and financial variables while retaining predictors that exhibit robust and consistent relationships with CPU dynamics. To this end, we apply four complementary screening techniques: Transfer Entropy, Granger Causality, Cross-Correlation analysis, and Wavelet Coherence. Detailed descriptions of

Table 4: Time series of the training samples for the three CPU indices, together with their ACF and PACF plots.



these methods and empirical results are provided in Appendix A. The screening procedures focus on the primary US CPU index developed by [37], which provides a sufficient number of observations to support reliable estimation of nonlinear dependencies, Granger causality, and wavelet coherence. This index therefore serves as the benchmark series for variable selection. Importantly, the temporal dynamics of the primary US and Global CPU indices remain closely aligned, as shown in Table 4, indicating that predictors identified using the US series are expected to capture relevant associations that extend beyond national boundaries. The alternative US CPU index is used as an additional robustness check, as its distinct volatility and persistence properties allow us to assess whether the selected predictors reflect structural drivers of US CPU rather than features tied to a specific index construction.

The four screening tests provide complementary perspectives on the associations between candidate variables and the CPU index. Transfer entropy captures nonlinear directional relationships and information flow, Granger Causality identifies short-run linear predictive dependencies, cross-correlation highlights lead-lag patterns and temporal synchronization, and wavelet coherence uncovers time- and frequency-specific co-movement, revealing how relationships evolve across scales. In terms of implementation, transfer entropy is applied in a pairwise framework as an initial screening device, Granger causality tests are conducted on the differenced series to ensure stationarity, since as the primary US CPU index is shown to be nonstationary in Table 3, and wavelet coherence is implemented using the “Morlet” mother wavelet with non-dimensional parameter specific to the wavelet function. Statistical significance is assessed via 100 Monte Carlo randomizations. Phase differences are plotted to capture lead-lag relationships across both time and frequency scales, and a representative example of the resulting coherence plots is shown in Fig. A.8 in Appendix A.5.

Variable retention follows a systematic rule designed to mitigate the effects of highly correlated predictors, reduce redundancy, and limit confounding effects arising from common macroeconomic factors. A variable is considered relevant if it is supported by at least two screening procedures, which reduces sensitivity to spurious associations. When multiple variables convey closely related economic information, only one representative series is retained to avoid redundancy and multicollinearity concerns. In such cases, preference is given to the variable exhibiting stronger and more consistent empirical support, measured by significance across a larger number of screening tests. For example, CES0600000008 (Average Hourly Earnings: Goods-Producing) and CES2000000008 (Average Hourly Earnings: Construction) capture wage dynamics within closely related segments of the goods-producing sector, with construction representing a subset of the broader goods-producing category. Consequently, they are influenced by similar labor market conditions and exhibit strong co-movement, leading to redundant information content. Hence, between CES0600000008 and CES2000000008, only the latter is retained, as it is supported by three screening procedures compared to two for the former. Finally, a very limited number of substantively important variables, such as the real S&P 500 index growth, are retained despite being supported by only one screening procedure, reflecting their well-established relevance in the macro-financial literature. This screening process yields a final set of 60 predictors that are used in the subsequent empirical analysis, with complete screening results reported in Appendix A.5.

4.2. Economic Relevance of Selected Predictors

This section provides a theoretical grounding for the macroeconomic and financial cycle variables included in the analysis, highlighting why they are expected to be systematically associated with movements in the CPU index. The goal is to ensure that the set of predictors selected through empirical screening is not only statistically robust but also economically meaningful. These variables capture the broader macro-financial environment that shapes policymakers' ability to implement, delay, or adjust environmental measures. CPU reflects the interplay of economic conditions, financial and credit constraints, and market sentiment, each of which can influence the timing, scope, and credibility of climate-related policies. By outlining these channels, this section establishes a clear economic rationale for the selected predictors, linking theoretical reasoning with the data-driven selection procedure.

Measures such as the business confidence index (BCI) and composite leading indicator (CLI) capture corporate forward-looking expectations about the economy and their readiness for additional investment. High BCI and CLI levels signal optimism about future growth, profitability, and policy stability. In such conditions, firms and investors perceive lower regulatory risk and are better able to anticipate and adapt to environmental policies. Conversely, when business confidence weakens, the economic environment becomes more uncertain, and firms tend to delay investment decisions, anticipating potential changes in policy direction. These results suggest that CPU is dependent on the state of the underlying economy [103]. Therefore, the inclusion of these indicators helps quantify the expectation-driven component of CPU, reflecting how economic sentiment conditions policy credibility and timing. Complementing these indicators, financial market variables further capture the real-time assessment of economic and policy risks by households and investors. Indicators such as the real S&P 500 index growth, cyclically adjusted price-to-earnings (CAPE) ratio, and credit growth represent the valuation and liquidity conditions underlying economic cycles. Rising equity prices and improving valuations generate a positive wealth effect, enhancing investor and household optimism. This optimism, in turn, lowers the perceived risk of stringent or abrupt policy changes, leading to a decline in CPU [28]. However, when asset valuations fall or credit conditions tighten, uncertainty about macroeconomic and regulatory prospects intensifies.

Housing market indicators, specifically total housing starts (HOUST) and new private housing permits in the northeastern US (PERMITNE), serve as forward-looking measures of construction sector vitality and real estate development. Periods of expansion in housing activity indicate confidence in long-term growth and reflect a robust macroeconomic environment conducive to policy experimentation. In such contexts,

households and firms exhibit greater adaptability to environmental regulations and are more likely to invest in climate-friendly technologies, such as energy-efficient housing and renewable installations. Conversely, contractions in housing activity, marked by lower permit issuance or construction starts, often coincide with economic downturns, prompting policymakers to delay or soften environmental measures to protect the real estate sector [28]. This relationship suggests that construction and housing-related indicators are likely to exert a stronger influence on CPU dynamics than sector-specific production variables such as manufacturing capacity utilization or mining employment.

The broader set of housing variables, including the household mortgage-to-income ratio, real house price growth (HPI), cyclically adjusted price-to-rent ratio (CAPR), and private residential fixed investment (PRFI), further elucidate the link between wealth dynamics, financial fragility, and policy sentiment. The mortgage-to-income ratio, in particular, reflects the amount of loans related to the financial stress of individual households due to home loan mortgages, which directly affect public sensitivity to policy reforms that could alter disposable income or asset values, thereby elevating CPU. In contrast, periods of stable or growing housing wealth, reflected by rising HPI or CAPR, tend to strengthen public support for climate-related reforms by reducing perceived financial risk. Hence, housing markets serve as transmission channels for both wealth and policy expectations, rendering them particularly sensitive to shifts in regulatory and macroeconomic conditions [78; 21].

Elevated household leverage imposes a binding political economy constraint on climate policy implementation. When household balance sheets are highly indebted, sensitivity to inflationary pressures increases, particularly those arising from climate policies such as carbon pricing or energy efficiency mandates that raise utility and compliance costs. In such environments, governments may delay implementation or issue ambiguous signals regarding the timing and scope of environmental regulations to prevent public backlash, thereby increasing CPU. Similarly, a high credit-to-GDP ratio suggests that the economy may be at the peak of a credit cycle, where financial institutions face heightened exposure to leverage and “stranded asset” risks. In such a scenario, policymakers must then balance decarbonization objectives against concerns over financial stability and credit conditions in carbon-intensive sectors, a trade-off that further amplifies uncertainty surrounding future climate policy actions.

The real personal consumption expenditures (DPCERA3M086SBEA as in Table A.10) provides insight into aggregate demand conditions, which are central to a consumption-driven economy such as that of the US. Strong consumption growth signals periods of economic expansion and rising public confidence, creating political space for stricter climate action. In contrast, subdued consumption reflects demand-side weakness, which often constrains the implementation of climate initiatives perceived as burdensome to households and firms [102]. Similarly, the personal interest payments-to-income ratio reflects household financial fragility and debt servicing pressures. Higher ratios indicate elevated leverage and reduced disposable income, which can heighten sensitivity to potential cost increases associated with carbon pricing or energy reforms. Thus, periods of rising household indebtedness are likely to coincide with heightened CPU, as policymakers face greater constraints in introducing or maintaining stringent climate measures. Finally, the unemployment rate embodies the trade-off between economic stability and environmental ambition. Elevated unemployment diverts public and political priorities toward immediate economic recovery, reducing tolerance for policies that could impose additional costs. This observation aligns with the findings of [61], who document that positive carbon policy shocks can depress aggregate output of the economy by 0.7% and raise inflation by 0.3%, reinforcing policymakers’ hesitation to advance environmental agendas during labor market stress.

These findings underscore the association between the selected predictors and the evolution of CPU, providing a theoretically informed perspective on their relationship with CPU. Business confidence and leading economic indicators capture expectation-driven uncertainty, while financial, housing, and credit variables trace the transmission of economic and wealth effects into policy credibility. Labor market and consumption measures reveal how economic conditions shape public support for environmental regulation. Overall, the results show that CPU arises from the interaction of economic sentiment, financial stability, and

public welfare expectations, underscoring that stabilizing economic expectations can mitigate climate-related policy uncertainty and strengthen long-term climate commitments.

4.3. Google Trends Indicators

Beyond macro-financial predictors, public attention and information diffusion also shape perceptions of climate policy. To capture this behavioral dimension, we incorporate data from “Google Trends”⁵ for a broad set of search terms related to climate policy. These include queries such as “climate policy”, “climate risk”, “environmental policy”, “carbon credits”, and “clean energy”, among others. All search terms are collected at the worldwide level; however, their temporal patterns closely mirror those of US-specific searches, as depicted in Fig. 1. The close alignment in both temporal patterns and magnitudes reflects the fact that global Google search intensity is heavily influenced by US policy developments and media coverage, which generate information shocks that dominate worldwide search dynamics. Additionally, global search terms are particularly relevant when forecasting the Global CPU index, which is also analyzed in this study. Consequently, retaining worldwide Google Trends series provides both a reasonable approximation for US behavior and valuable predictive information for CPU.

Incorporating Google Trends data complements macroeconomic and financial indicators by introducing a social attention component, capturing shifts in public concern, awareness, and anticipation of policy initiatives. Fig. 2 shows clear co-movement between public search behavior and the primary US CPU index, indicating that CPU is influenced not only by economic and policy conditions but also by shifts in collective perception and information flow. A surge in search activity may correspond to heightened discourse around policy developments or global climate events, such as United Nations climate conferences, which are associated with elevated CPU levels. Conversely, declining search interest can signal stabilization in policy expectations. Although Google Trends provides a valuable proxy for public attention, it can exhibit temporal spikes unrelated to substantive policy changes, introducing potential measurement noise. To address this, we apply the four screening techniques described in Section 4.1 to identify search terms that display robust and consistent co-movement with the primary US CPU index. Only these significant terms are retained for inclusion in the forecasting model, and they are listed in Table A.11 in Appendix A.5.

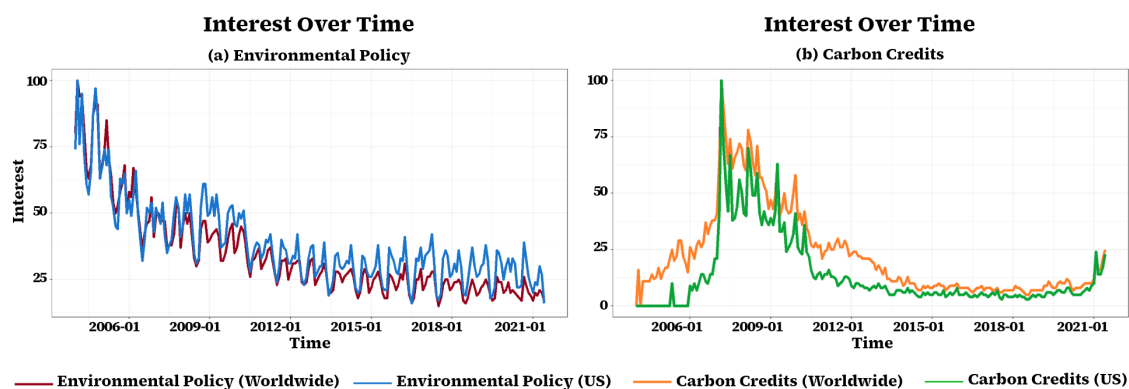


Figure 1: Global and US interest in the Google search terms (a) “Environmental Policy” and (b) “Carbon Credits” from January 2004 to June 2021. The series display similar temporal patterns, highlighting the close alignment between US and worldwide search behavior. Data sourced from Google Trends: <https://trends.google.com/trends?geo=US&hl=en-GB>.

⁵<https://trends.google.com/trends?geo=US&hl=en-GB>.

Interest Over Time

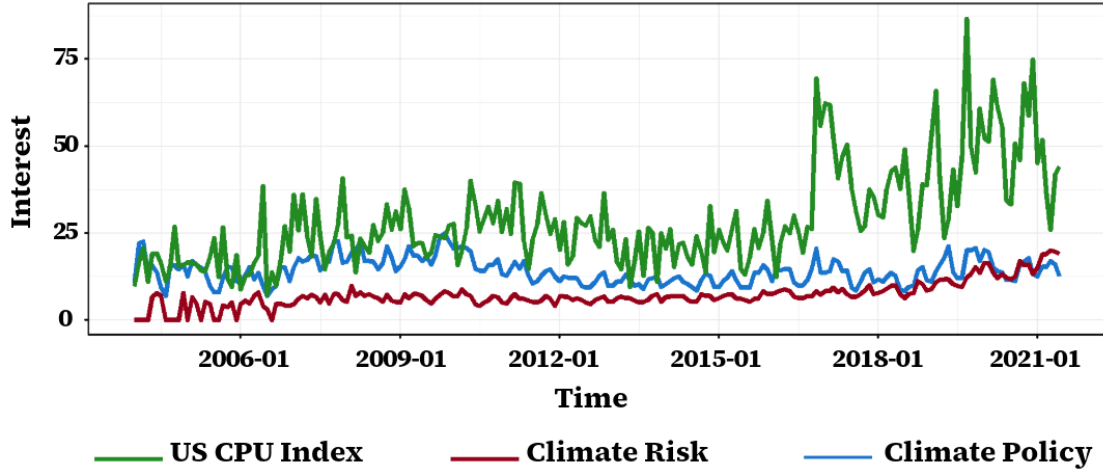


Figure 2: Interest in the worldwide search terms “Climate Policy” and “Climate Risk” from January 2004 to June 2021, plotted alongside the primary US CPU index. The three series exhibit similar temporal patterns.

5. Model Formulation

The Bayesian Structural Time Series (BSTS) model, introduced by [89], provides a flexible approach for forecasting time series data that extends the classical structural time series model by incorporating Bayesian inference to jointly estimate the model parameters and unobserved components. First, the observed series y_t is decomposed into latent components such as trends, seasonal fluctuations, and the influence of external covariates. Each component is specified within a state-space formulation, which provides a systematic way to model their evolution over time. The Bayesian framework enables the inclusion of prior knowledge, which is beneficial in managing uncertainty about model specification and producing forecasts along with their associated uncertainty through the posterior distribution. This combination makes BSTS particularly useful in economic forecasting problems, where interpretability, rigorous uncertainty assessment, and the integration of diverse economic and sentiment indicators are crucial.

The BSTS framework relies on the state-space representation, where the observed time series y_t is associated with an unobserved state vector α_t . This formulation uses the idea that the observable data are generated by latent processes evolving over time. The general form of a state-space model is expressed as:

$$\begin{aligned} y_t &= Z_t^\top \alpha_t + \epsilon_t, & \epsilon_t &\sim \mathcal{N}(0, H_t) \\ \alpha_{t+1} &= T_t \alpha_t + R_t \eta_t, & \eta_t &\sim \mathcal{N}(0, Q_t), \end{aligned} \quad (1)$$

where y_t denotes the observed time series, α_t represents the latent state vector encompassing the unobserved components of the model. The matrices Z_t and T_t are the observation and transition matrices, respectively. The observation matrix Z_t links the unobserved states to the observed data, while the transition matrix T_t describes how the unobserved states change over time. The terms ϵ_t and η_t are independent and identically distributed Gaussian noise processes with covariance matrices H_t and Q_t , respectively, reflecting observation and state uncertainties. We consider the observation noise covariance H_t to be a positive scalar, denoted by σ_ϵ^2 , following the specification in [89]. The components of the BSTS framework are detailed in Appendix B. Together, these components allow the BSTS model to flexibly capture the diverse patterns and dynamics characteristic of macroeconomic time series.

5.1. Prior Specification

To handle high-dimensional data, the BSTS model employs the spike and slab prior to induce sparsity by effectively setting most regression coefficients to zero while allowing a subset to vary. This is relevant for CPU forecasting due to the strong association between CPU and a large number of potential macroeconomic and financial cycle variables. This approach begins by introducing an indicator variable γ_k encoding whether predictor x_k is included in the model:

$$\gamma_k = \begin{cases} 1, & \text{if } \beta_k \neq 0 \\ 0, & \text{if } \beta_k = 0, \end{cases}$$

where β_k is the coefficient of predictor x_k . Then, we define β_γ as the vector of regression coefficients corresponding to predictors with $\gamma_k = 1$. The joint prior over the coefficients β , indicator vector γ , and observation noise variance σ_ϵ^2 , namely the “spike and slab” prior, is formulated as follows:

$$p(\beta, \gamma, \sigma_\epsilon^2) = p(\beta_\gamma | \gamma, \sigma_\epsilon^2) p(\sigma_\epsilon^2 | \gamma) p(\gamma).$$

The marginal prior $p(\gamma)$, referred to as the “spike”, assigns high probability to zero coefficients for irrelevant predictors, thereby encouraging sparsity. For computational convenience, each γ_k is assumed to follow an independent Bernoulli distribution:

$$\gamma \sim \prod_{k=1}^K \pi_k^{\gamma_k} (1 - \pi_k)^{1 - \gamma_k},$$

where π_k represents the prior inclusion probability of predictor x_k . In practice, all π_k are set to a common value $\pi = \frac{\tilde{p}}{K}$, defined as the expected model size, with \tilde{p} being the expected number of nonzero predictors and K is the total number of predictors. The “slab” corresponds to the conditional conjugate priors on the included coefficients and the variance, $p(\beta_\gamma | \sigma_\epsilon^2, \gamma)$ and $p(\frac{1}{\sigma_\epsilon^2} | \gamma)$, respectively. They are modeled as:

$$\beta_\gamma | \sigma_\epsilon^2, \gamma \sim \mathcal{N}\left(b_\gamma, \sigma_\epsilon^2 (\Omega_\gamma^{-1})^{-1}\right), \quad \frac{1}{\sigma_\epsilon^2} | \gamma \sim \text{Gamma}\left(\frac{\nu}{2}, \frac{ss}{2}\right),$$

where b_γ represents the prior mean vector, Ω_γ^{-1} is a symmetric matrix corresponding to $\gamma_k = 1$, and ν and ss denote the expected coefficient of variation (R^2) from the regression and the prior sample size, respectively. The precision matrix Ω_γ^{-1} is defined as $\Omega_\gamma^{-1} = \kappa(\omega X^\top X + (1 - \omega) \text{diag}(X^\top X))/n$, where X is the design matrix, n is the total number of observations, and κ represents the number of significance observations on the prior mean $b_\gamma = 0$, with $\omega = \frac{1}{2}$ and $\kappa = 1$, following [89]. This formulation enables the model to select the most relevant predictors for the observed time series while excluding irrelevant predictors.

5.2. Posterior Distribution

In Bayesian inference, the posterior distribution reflects the updated beliefs about model parameters after incorporating the observed data. This is especially valuable in economic applications, where uncertainty and prior knowledge play a critical role in inference and forecasting. In order to derive the posterior distribution, we first define θ as the set of model parameters, excluding the regression coefficients β and the observation noise variance σ_ϵ^2 . The posterior distribution $p(\theta | y)$ is given by Bayes’ theorem as:

$$p(\theta | y) = \frac{p(y | \theta) p(\theta)}{p(y)},$$

where $p(y | \theta)$ is the likelihood of the observed data given the parameters θ , $p(\theta)$ is the prior belief about the parameters before observing the data, and $p(y)$ is the marginal likelihood, acting as a normalizing constant, obtained by integrating out all the parameters. In order to facilitate posterior inference, the observed series is transformed to separate the contributions of the latent state α_t from those of the covariates by defining $\mathbf{y}_t^* = y_t - Z_t^{*\top} \alpha_t$, where

$Z_t^{*\top}$ is the observation matrix from Eqn. (1) with the regression term $\beta^\top x_t$ excluded. Given an inclusion vector γ , the conditional posterior distributions for the regression coefficients β_γ and noise variance σ_ϵ^2 are modeled as:

$$\beta_\gamma \mid \sigma_\epsilon^2, \gamma, \mathbf{y}^* \sim \mathcal{N}(\tilde{\beta}_\gamma, \sigma_\epsilon^2 (V_\gamma^{-1})^{-1}), \quad \frac{1}{\sigma_\epsilon^2} \mid \gamma, \mathbf{y}^* \sim \text{Gamma}\left(\frac{N}{2}, \frac{SS_\gamma}{2}\right).$$

Following the specifications of [89], the matrix $V_\gamma^{-1} = (X^\top X)_\gamma + \Omega_\gamma^{-1}$. The posterior mean of the regression coefficients for the selected variables $\tilde{\beta}_\gamma = (V_\gamma^{-1})^{-1} (X_\gamma^\top \mathbf{y}^* + \Omega_\gamma^{-1} b_\gamma)$. The sample size N combines the observed sample size n and the prior sample size ν , i.e., $N = n + \nu$, and the adjusted sum of squares is given by $SS_\gamma = ss + \mathbf{y}^{*\top} \mathbf{y}^* + b_\gamma^\top \Omega_\gamma^{-1} b_\gamma - \tilde{\beta}_\gamma^\top V_\gamma^{-1} \tilde{\beta}_\gamma$. Intuitively, these expressions update the prior distribution of the regression coefficients β_γ by integrating information from the observed data, represented by $X^\top X$, with prior knowledge encoded in the precision matrix Ω_γ^{-1} and mean vector b_γ . The resulting posterior reflects a weighted balance between the data likelihood and prior beliefs. Subsequently, the marginal posterior distribution for γ , which determines which predictors are included, is given by:

$$\gamma \mid \mathbf{y}^* \sim C(\mathbf{y}^*) \frac{|\Omega_\gamma^{-1}|^{\frac{1}{2}} p(\gamma)}{|V_\gamma^{-1}|^{\frac{1}{2}} SS_\gamma^{\frac{N}{2}-1}},$$

where $C(\mathbf{y}^*)$ is a normalizing constant that is independent of γ . The posterior distribution of the BSTS model is difficult to compute explicitly due to its high dimensionality and highly structured dependencies. However, it can be approximated using a Markov Chain Monte Carlo algorithm with the following steps:

1. Sample the latent state α from $p(\alpha \mid y, \theta, \beta, \sigma_\epsilon^2)$ using the simulation smoother of [32]. This step accounts for the unobserved time-varying components such as trend and seasonality.
2. Sample the parameters θ from $p(\theta \mid y, \alpha, \beta, \sigma_\epsilon^2)$, updating beliefs about the components.
3. Sample the regression coefficients β and variance σ_ϵ^2 from a Markov chain with the stationary distribution $p(\beta, \sigma_\epsilon^2 \mid y, \alpha, \theta)$.

Setting $\phi = (\theta, \beta, \sigma_\epsilon^2, \alpha)$, the procedure could be iterated to produce samples $\phi^{(1)}, \phi^{(2)}, \dots$, which converge in distribution to the true posterior $p(\phi \mid y)$ [89].

6. Experimental Analysis

This section evaluates the forecasting performance of the BSTS model for multiple measures of CPU, including the primary US CPU index, the alternative US CPU index, and the Global CPU index, and investigates the economic significance of the variables identified by the model. We compare the BSTS performance against benchmark statistical, machine learning, and deep learning forecasting models across four time horizons: 3-month-ahead, 6-month-ahead, 12-month-ahead, and 24-month-ahead, to assess its adaptability and robustness. This section is organized as follows. Sections 6.1 and 6.2 provide concise overviews of the baseline models and the evaluation metrics, respectively. Section 6.3 details the experimental results and benchmark comparisons. Section 6.4 discusses the statistical significance of the forecasts. Section 6.5 provides an ablation study of BSTS models with time-invariant and time-varying coefficients to evaluate the impact of coefficient flexibility on forecasting performance. Section 6.6 examines the responses of the CPU index to innovations in key macroeconomic and financial cycle variables, providing empirical support for the theoretical channels discussed in Sections 2 and 4.2. Section 6.7 complements this analysis by presenting the feature importance plot, highlighting the economic relevance of the variables selected by the BSTS model. Finally, Section 6.8 presents the credible intervals generated by the BSTS model.

6.1. Baseline Models

The forecasting performance of the BSTS model is evaluated against a range of statistical, machine learning, and deep learning models, all of which can incorporate covariates. The benchmark frameworks include: Autoregressive Integrated Moving Average with exogenous variables (ARIMA-X), Autoregressive Fractionally Integrated

Moving Average with exogenous variables (ARFIMA-X), Autoregressive Neural Network with exogenous variables (ARNN-X), Neural Basis Expansion Analysis for Time Series with exogenous variables (NBeats-X), Neural Hierarchical Interpolation for Time Series with exogenous variables (NHITS-X), Decomposition-based Linear model with exogenous variables (DLinear-X), and Normalization-based Linear model with exogenous variables (NLinear-X). A comprehensive overview of these baseline models can be found in Appendix C.1.

6.2. Evaluation Metrics

Five evaluation metrics are employed to assess the forecasting performance of the competing models. These metrics include Root Mean Squared Error (RMSE), Mean Absolute Error (MAE), Mean Absolute Scaled Error (MASE), Mean Absolute Percentage Error (MAPE), and Symmetric Mean Absolute Percentage Error (SMAPE). These metrics are chosen to provide a comprehensive assessment of forecast accuracy, capturing both absolute and relative errors, sensitivity to large deviations, and scale-independent performance. Their mathematical formulations are given by:

$$\begin{aligned} \text{RMSE} &= \sqrt{\frac{1}{h} \sum_{t=1}^h (y_t - \hat{y}_t)^2}; & \text{MASE} &= \frac{\sum_{t=1}^h |\hat{y}_t - y_t|}{\frac{h-1}{T-1} \sum_{t=2}^T |y_t - y_{t-1}|}; & \text{MAE} &= \frac{1}{h} \sum_{i=1}^h |y_i - \hat{y}_i|; \\ \text{MAPE} &= \frac{1}{h} \sum_{t=1}^h \frac{|\hat{y}_t - y_t|}{|y_t|} \times 100\%; & \text{SMAPE} &= \frac{1}{h} \sum_{t=1}^h \frac{|\hat{y}_t - y_t|}{(|\hat{y}_t| + |y_t|)/2} \times 100\%, \end{aligned}$$

where y_t represents the observed time series, \hat{y}_t is the forecasted value, h refers to the forecast horizon, and T is the length of the in-sample (training) period. According to standard practice, the model with the lowest error metric is regarded as the best-performing model [50].

6.3. Experimental Results and Baseline Comparison

To ensure a comprehensive evaluation, the BSTS model is compared against several state-of-the-art forecasters. The implementation of the BSTS model is carried out in **R** statistical software using the `bsts` function of the `bsts` package. The benchmark models ARIMA, ARFIMA, and ARNN are implemented through the `forecast` package, while the deep learning models NBeats, NHITS, DLinear, and NLinear are implemented via Python’s `darts` library. Model estimation and forecast evaluation are conducted within a consistent and leakage-free empirical framework. For each forecast horizon h , models are trained on all available observations except the last h points, which are reserved as the test set. Hyperparameters are selected using only information available in the training sample. Out-of-sample forecasts are then generated recursively for the test set, ensuring that only information available at time t is used in prediction. All predictors are similarly constructed using information available at time t , maintaining a consistent real-time forecasting setup. This procedure is applied separately for each forecast horizon, with the test set length and corresponding training window defined by the horizon. The splitting scheme is summarized in Table 5, providing a transparent description of the forecast evaluation design. The optimal state specifications of the BSTS model, selected by minimizing the RMSE metric, are listed in Table 6.

Table 5: Training and testing periods for forecasting CPU indices across different forecast horizons.

CPU Index	Horizon	Training Period	Number of Observations	Testing Period	Number of Observations
Primary (US)	$h = 3$	Apr 1987 - Mar 2023	432	Apr 2023 - Jun 2023	3
	$h = 6$	Apr 1987 - Dec 2022	429	Jan 2023 - Jun 2023	6
	$h = 12$	Apr 1987 - Jun 2022	423	Jul 2022 - Jun 2023	12
	$h = 24$	Apr 1987 - Jun 2021	411	Jul 2021 - Jun 2023	24
Alternative (US) & Global	$h = 3$	Jan 2000 - Mar 2023	279	Apr 2023 - Jun 2023	3
	$h = 6$	Jan 2000 - Dec 2022	276	Jan 2023 - Jun 2023	6
	$h = 12$	Jan 2000 - Jun 2022	270	Jul 2022 - Jun 2023	12
	$h = 24$	Jan 2000 - Jun 2021	258	Jul 2021 - Jun 2023	24

Excluding covariates from the forecasting framework undermines the economic interpretability and structural validity of the model. As discussed in Section 2, macroeconomic and financial cycle indicators serve as fundamental predictors of the CPU index, capturing key economic linkages and transmission mechanisms that shape climate-related policy uncertainty. Their inclusion enhances the model’s ability to reflect underlying structural dynamics,

Table 6: Optimal BSTS state specifications for forecasting the three CPU indices across different forecast horizons. Notation: LL = Local Level, LLT = Local Linear Trend, AR = Autoregressive component, S = Seasonal component.

CPU Index	$(state\ specification)_{h=3}$	$(state\ specification)_{h=6}$	$(state\ specification)_{h=12}$	$(state\ specification)_{h=24}$
Primary (US)	LL, AR, S	LLT, AR, S	LLT	LL, LLT, AR, S
Alternative (US)	LLT	LLT, S	LLT	LL, AR, S
Global	AR	LL, AR	LL, AR	LLT, AR, S

ensuring that forecasts remain both theoretically consistent and practically informative for economic analysis and decision-making. Therefore, this study focuses on evaluating the additional predictive power gained from incorporating sentiment information. To do this, all models are estimated under two distinct configurations: (i) including the 60 statistically significant macroeconomic and financial cycle indicators (denoted as X_M), and (ii) including both the 60 macro-financial variables together with sentiment-based data derived from Google Trends (denoted as X_{MG}). This setup enables a systematic comparison of the forecasting performance across both covariate sets.

After implementing BSTS and the baseline models, out-of-sample forecasts were generated for multiple horizons (3-, 6-, 12-, and 24-month-ahead) using the two covariate sets (X_{MG} and X_M). Forecasts are generated recursively, with multi-step-ahead predictions obtained sequentially from earlier forecasts, thereby ensuring a realistic assessment of model performance across horizons. For the primary US CPU index, Tables 7 and 8 report the predictive performance on the test set using the sets X_{MG} and X_M , respectively. The results indicate that ARFIMA achieves the highest accuracy for short-term forecasts, corresponding to the 3-month-ahead horizon ($h = 3$), across both covariate sets, followed closely by BSTS. However, BSTS consistently outperforms all baseline models over the medium- and long-term horizons, corresponding to the 6-, 12-, and 24-month-ahead horizons ($h = 6, 12, 24$, respectively), reflecting its ability to capture persistent temporal dependencies that are particularly relevant for climate policy and investment decisions as they typically unfold over extended periods. The superior performance of BSTS can be attributed to its spike-and-slab prior, which effectively identifies the most informative predictors while excluding irrelevant covariates, thereby reducing model complexity, mitigating overfitting, and allowing the model to adapt dynamically to evolving relationships within the data. Importantly, our pre-model variable selection procedure complements this Bayesian regularization by retaining variables with consistent empirical support across multiple screening methods, which mitigates the risk of posterior probability dilution among highly correlated predictors, ensuring that the posterior distribution concentrates on truly relevant predictors. Notably, the inclusion of Google Trends indicators in X_{MG} consistently improves BSTS performance relative to X_M , highlighting the added informational value of behavioral indicators in forecasting CPU.

The performance of the models on the test set for the alternative US CPU index is reported in Appendix C.2, Tables C.12 and C.13, corresponding to the covariate sets X_{MG} and X_M , respectively. Using the set X_{MG} , BSTS and ARIMA exhibit the strongest accuracy at the 3-month-ahead horizon, depending on the evaluation metric, while ARIMA slightly outperforms BSTS at the 6-month horizon. For the 12-month-ahead horizon, ARNN achieves the highest predictive performance. When using the set X_M , BSTS and NLinear perform best at the 3-month horizon, whereas ARFIMA delivers superior accuracy at both the 6- and 12-month horizons. Importantly, BSTS demonstrates the strongest performance at the 24-month-ahead horizon across both covariate sets, which remains the most relevant time frame for informing climate policy and decision-making. During the implementation of ARIMA and ARFIMA, a small number of Google Trends indicators were omitted to ensure model convergence.

For the Global CPU index, model performance using the covariate sets X_{MG} and X_M on the test set is reported in Appendix C.2, Tables C.14 and C.15, respectively. BSTS attains the highest accuracy for the 3- and 6-month-ahead horizons, while at 12 months its performance is comparable to ARNN, depending on the evaluation metric when using the set X_{MG} . However, when using the set X_M , short-term accuracy at the 3-month horizon varies across metrics, with BSTS and NLinear performing well, whereas the leading models at the 6- and 12-month horizons differ by metric. Notably, BSTS consistently demonstrates strong predictive performance across both covariate sets at the 24-month-ahead horizon. Hence, the US macroeconomic and financial cycle variables identified from the primary US CPU index encapsulate meaningful and transferable information that is also predictive of Global CPU. This outcome provides empirical support for the variable selection strategy adopted in Section 4.1. Moreover, it confirms the applicability of BSTS to forecasting CPU indices beyond the US context, indicating that its predictive advantages are not confined to a single national index. While BSTS is capable of handling large sets of covariates, alternative statistical models lack this capacity. Conversely, neural network architectures are black-box models, limiting their

applicability in high-stakes decision-making settings where interpretability is desired.

Several notable patterns emerge from the combined results. First, BSTS consistently achieves superior performance at the 24-month-ahead horizon across all indices and covariate sets, underscoring its relevance for long-term climate policy planning. Second, the inclusion of Google Trends indicators markedly enhances BSTS performance, highlighting the value of incorporating public attention and information diffusion into the forecasting framework. Finally, a similar, though less pronounced, improvement is observed for the statistical and machine learning models, suggesting that sentiment-based data can enhance their predictive ability. In contrast, the performance of deep learning models generally declines as the dimensionality of the covariates increases. This limitation is attributed to the absence of an explicit variable selection mechanism, combined with the relatively limited number of observations of the CPU index series, which introduces additional noise and hinders the models’ ability to learn stable patterns. Hence, excluding these additional variables mitigates the risk of overfitting, thus enhancing the accuracy of these models. By comparison, BSTS does not suffer from this degradation, as its spike-and-slab prior enables variable selection and shrinkage, preventing noise accumulation even in high-dimensional covariate spaces. Taken together, these findings underscore both the empirical and policy relevance of the BSTS framework and the central role of macro-financial conditions and sentiment-based Google Trends indicators in shaping the dynamics of CPU.

Table 7: Evaluation of the BSTS- X_{MG} model’s performance relative to baselines across all forecast horizons for the primary US CPU index using macro-financial variables and Google Trends indicators. The **best** and *second-best* results are highlighted.

Horizon	Metric	ARFIMA- X_{MG}	ARIMA- X_{MG}	ARNN- X_{MG}	BSTS- X_{MG}	NBEATS- X_{MG}	NHiTS- X_{MG}	DLinear- X_{MG}	NLinear- X_{MG}
$h = 3$	MAPE	2.381	14.147	9.368	<i>4.708</i>	50.601	16.053	35.628	22.305
	SMAPE	2.329	13.582	9.317	<i>4.598</i>	39.630	14.401	29.489	19.806
	MAE	5.346	32.034	20.996	<i>10.568</i>	112.928	35.616	79.831	49.823
	MASE	0.919	5.507	3.610	<i>1.817</i>	19.415	6.123	13.724	8.566
	RMSE	7.384	38.779	21.123	<i>10.655</i>	118.719	42.559	87.526	53.186
$h = 6$	MAPE	16.299	10.896	<i>8.186</i>	6.029	55.015	31.979	33.733	24.987
	SMAPE	18.155	11.424	<i>8.455</i>	6.343	41.896	26.388	28.258	21.895
	MAE	40.330	26.575	<i>20.230</i>	5.572	129.318	72.532	77.783	57.627
	MASE	1.372	0.904	<i>0.688</i>	0.530	4.401	2.468	2.647	1.961
	RMSE	47.209	33.874	<i>25.702</i>	24.201	139.230	84.355	83.300	61.294
$h = 12$	MAPE	18.605	19.187	<i>13.795</i>	11.345	74.528	43.596	28.088	27.713
	SMAPE	21.217	21.530	<i>15.295</i>	12.133	52.193	34.688	25.878	25.423
	MAE	47.620	48.585	<i>36.038</i>	29.361	164.626	96.759	67.963	66.540
	MASE	1.365	1.393	<i>1.033</i>	0.842	4.719	2.774	1.948	1.907
	RMSE	59.830	66.708	<i>59.739</i>	44.153	177.004	107.107	87.748	82.833
$h = 24$	MAPE	36.951	27.282	<i>24.502</i>	18.194	32.408	34.603	36.579	29.985
	SMAPE	44.414	32.126	<i>26.489</i>	19.182	32.406	39.809	42.008	33.742
	MAE	90.807	69.591	<i>59.253</i>	44.670	81.390	89.026	89.146	77.392
	MASE	1.479	1.134	<i>0.965</i>	0.728	1.326	1.450	1.452	1.261
	RMSE	103.194	91.093	<i>77.387</i>	66.440	109.319	116.036	112.517	102.789

6.4. Robustness and Statistical Significance Tests

The forecasting performance of the competing models is evaluated using the model-agnostic Multiple Comparisons with the Best (MCB) procedure to assess the statistical significance of differences in measurement errors. The MCB test is a nonparametric ranking approach that orders each of the \mathcal{M} forecasting models based on their predictive accuracy across \mathcal{D} datasets [59]. The model with the lowest average rank is identified as the best-performing forecasting framework. Fig. 3 depicts the ranking of the models across the three CPU indices for the two covariate configurations. The BSTS- X_{MG} model achieves the lowest mean rank of 2.50 under the RMSE metric across all forecast horizons, establishing it as the top-performing model, followed by BSTS- X_M (3.08), and ARIMA- X_{MG} (5.42). The MCB results indicate that BSTS- X_M performs comparably but does not outperform BSTS- X_{MG} , underscoring the value of incorporating both macro-financial indicators and Google Trends data when forecasting the CPU index.

The gray-shaded region in Fig. 3 represents the upper limit of the critical distance for BSTS- X_{MG} , serving as the benchmark for comparison. The deep learning models NHiTS, NBEATS, and DLinear exhibit critical intervals well above this threshold, signifying substantially weaker forecasting performance mainly due to the limited size of the training data. Consistent with the results reported in Section 6.3, models such as ARIMA, ARFIMA, and ARNN

Table 8: Evaluation of the $BSTS-X_M$ model’s performance relative to baselines across all forecast horizons for the primary CPU index using macro-financial variables. The **best** and **second-best** results are highlighted.

Horizon	Metric	ARFIMA- X_M	ARIMA- X_M	ARNN- X_M	BSTS X_M	NBEATS- X_M	NHiTS- X_M	DLinear- X_M	NLinear- X_M
h = 3	MAPE	2.388	10.108	8.991	<i>4.597</i>	39.965	21.413	6.777	5.473
	SMAPE	2.328	10.732	9.498	<i>4.493</i>	32.744	19.306	6.576	5.586
	MAE	5.403	22.617	20.334	<i>10.316</i>	89.059	47.878	15.038	12.401
	MASE	0.929	3.888	3.496	<i>1.774</i>	15.311	8.231	2.585	2.132
	RMSE	7.983	24.992	22.719	<i>10.384</i>	93.807	48.287	16.838	14.689
h = 6	MAPE	16.299	15.348	<i>8.530</i>	6.218	78.979	12.845	9.379	8.825
	SMAPE	18.155	16.959	8.740	6.514	55.271	13.812	9.374	<i>8.526</i>
	MAE	40.330	37.013	<i>17.144</i>	15.959	182.182	31.902	22.284	20.990
	MASE	1.372	1.260	<i>0.583</i>	0.543	6.200	1.086	0.758	0.714
	RMSE	47.209	41.596	<i>23.012</i>	24.372	190.497	43.951	24.206	23.723
h = 12	MAPE	18.713	19.391	<i>18.233</i>	13.109	82.676	31.806	23.715	19.439
	SMAPE	21.355	22.730	21.689	13.250	57.214	27.998	22.313	<i>18.159</i>
	MAE	47.885	50.231	47.810	31.904	185.336	72.103	55.801	<i>45.274</i>
	MASE	1.373	1.440	1.371	0.915	5.313	2.067	1.600	<i>1.298</i>
	RMSE	60.100	66.534	68.297	41.903	195.770	85.485	70.668	<i>56.954</i>
h = 24	MAPE	36.951	30.759	29.900	21.491	31.907	47.433	26.375	<i>25.637</i>
	SMAPE	44.414	36.677	34.549	23.382	35.416	43.404	28.479	29.233
	MAE	90.807	77.414	72.859	53.364	81.261	113.077	67.907	<i>67.646</i>
	MASE	1.479	1.261	1.187	0.869	1.324	1.842	1.106	<i>1.102</i>
	RMSE	103.194	95.410	<i>88.810</i>	72.952	111.822	134.613	91.364	94.302

demonstrate improved accuracy when the covariate set X_{MG} is employed, whereas deep learning architectures tend to deteriorate with the inclusion of additional predictors. This divergence is likely attributed to their increased susceptibility to noise and overfitting in high-dimensional settings, as well as the limited number of observations in some CPU index series, which restricts their capacity to reliably learn complex relationships from a high-dimensional set of exogenous variables. Overall, the MCB analysis confirms statistically significant differences in model performance and provides further evidence that the BSTS framework consistently outperforms alternative models across different forecast horizons.

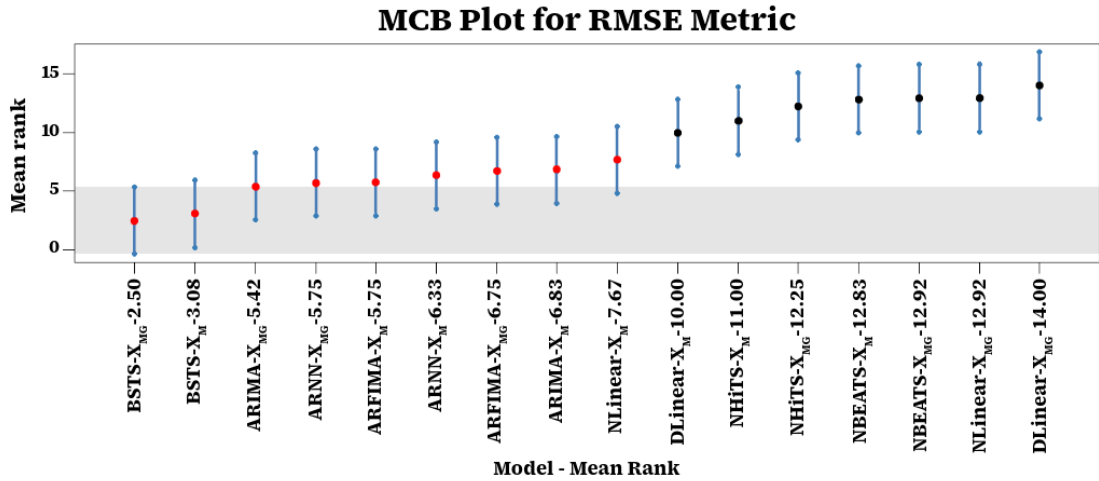


Figure 3: Multiple comparisons with the best (MCB) plot comparing model performance across the two covariate sets and the three CPU indices. $BSTS-X_{MG}-2.50$, for instance, signifies that the average ranking of the $BSTS-X_{MG}$ model, according to the RMSE metric, is 2.50. This same interpretation holds for other models.

From Fig. 3, we observe that $BSTS-X_{MG}$ achieves higher predictive performance than $BSTS-X_M$; nonetheless, the difference is marginal. To further demonstrate the substantial explanatory power and forecasting improvement gained from incorporating sentiment-based Google Trends indicators, we employ the Murphy diagram analysis. Unlike the MCB procedure, which ranks models based on their average forecast accuracy, the Murphy diagram evaluates whether a model consistently outperforms competing alternatives across a wide family of scoring functions

[33; 24]. This approach provides a more comprehensive assessment of the robustness of forecast performance. The Murphy diagram is constructed using the following scoring function:

$$\tilde{s}(\hat{y}_t, y_t) = \begin{cases} |y_t - \theta|, & \min(\hat{y}_t, y_t) \leq \theta < \max(\hat{y}_t, y_t) \\ 0, & \text{otherwise,} \end{cases} \quad (2)$$

where y_t denotes the observed value at time t , and \hat{y}_t is the forecast generated by the model. The parameter $\theta \in \mathbb{R}$ determines the shape of the loss function and acts as a threshold sliding between the forecast and the observation, thereby enabling the scoring function to highlight different aspects of forecast errors. Specifically, lower values of θ increase the penalty for underestimations, while higher values place greater weight on overestimations. To assess the relative performance of competing forecasting models, the average score for model i over a forecast horizon of length h is computed as $\mathcal{S}_i(\theta) = \frac{1}{h} \sum_{t=1}^h \tilde{s}(\hat{y}_{t,i}, y_t)$, where $\hat{y}_{t,i}$ is the forecast from model i at time t . Plotting the average scores $\mathcal{S}_i(\theta)$ across a range of values of θ yields the Murphy diagram. Consequently, the Murphy diagram serves as a flexible and insightful tool to identify models that consistently outperform others across diverse scoring functions. To empirically assess the robustness of the BSTS- X_{MG} model relative to benchmark methods, we use the `murphydiagram` package in **R** to construct Murphy diagrams for all three CPU indices. Murphy diagrams compare BSTS- X_{MG} against BSTS- X_M and ARIMA- X_{MG} , the strongest competing models according to the RMSE-based MCB test.

Fig. 4 presents the Murphy diagrams for the 24-month-ahead horizon. Lower extremal scores indicate superior predictive accuracy. The results for both the US CPU indices indicate that BSTS- X_{MG} consistently outperforms BSTS- X_M and ARIMA- X_{MG} across a broad range of values for θ , with the performance gap being particularly pronounced for low to mid-range thresholds. This outcome reinforces the findings of the MCB analysis and underscores the significant forecasting value of integrating sentiment-based Google Trends indicators. In contrast, for the Global CPU index, the performance differential between BSTS- X_{MG} and BSTS- X_M is negligible across the range of θ values considered. This suggests that, at the global level, Google Trends variables provide little incremental predictive value beyond macro-financial covariates. Fig. 4 further demonstrates that BSTS consistently outperforms ARIMA across all CPU indices, providing empirical support for the Bayesian model’s superior long-horizon forecasting ability. The relative advantage of BSTS- X_{MG} , however, diminishes when θ exceeds approximately 225 for the primary US CPU index, 4 for the alternative US CPU index, and 160 for the Global CPU index, indicating that performance differences narrow when overprediction penalties dominate. By combining insights from both the MCB and Murphy analyses, we establish robust evidence of the forecasting superiority of the BSTS framework and the substantial predictive contribution of Google Trends indicators in forecasting CPU indices.

6.5. Ablation Study: Time-Invariant versus Time-Varying Regression Coefficients

The policy-sensitive nature of the CPU index raises the question of whether allowing regression coefficients to evolve over time improves forecasting performance, as assuming time-invariant coefficients in this context implicitly limits the ability to capture structural changes and interpret policy-driven dynamics. To validate this, we conducted an ablation study comparing BSTS models with time-invariant coefficients (BSTS- X_{MG}^{TI}) against models with time-varying coefficients (BSTS- X_{MG}^{TV}), using the optimal state-space specifications reported in Table 6 and the covariate set X_{MG} , which was identified in Sections 6.3 and 6.4 as most predictive. Results for all CPU indices and forecast horizons are reported in Table 9.

The results shows that BSTS with time-invariant coefficients consistently outperforms the time-varying specification. For the primary US CPU index, BSTS- X_{MG}^{TI} achieves superior accuracy across all horizons. For the alternative US and Global CPU indices, BSTS- X_{MG}^{TV} only surpasses the time-invariant model at the 6- and 12-month horizons, respectively, while BSTS- X_{MG}^{TI} provides better forecasts for all remaining horizons. The superior performance of the BSTS model with time-invariant coefficients can be attributed to two key factors. First, several CPU index series have a limited number of observations, constraining the ability of BSTS- X_{MG}^{TV} to learn stable patterns, particularly when combined with a large set of covariates. Second, the covariate set X_{MG} already captures the most relevant macro-financial and behavioral information, reducing the need for additional flexibility in the regression coefficients. Hence, fixing the coefficients mitigates the risk of overfitting, ensuring more robust long-horizon predictions. These findings indicate that, for the CPU index, incorporating time-varying regression coefficients is not effective. Conse-

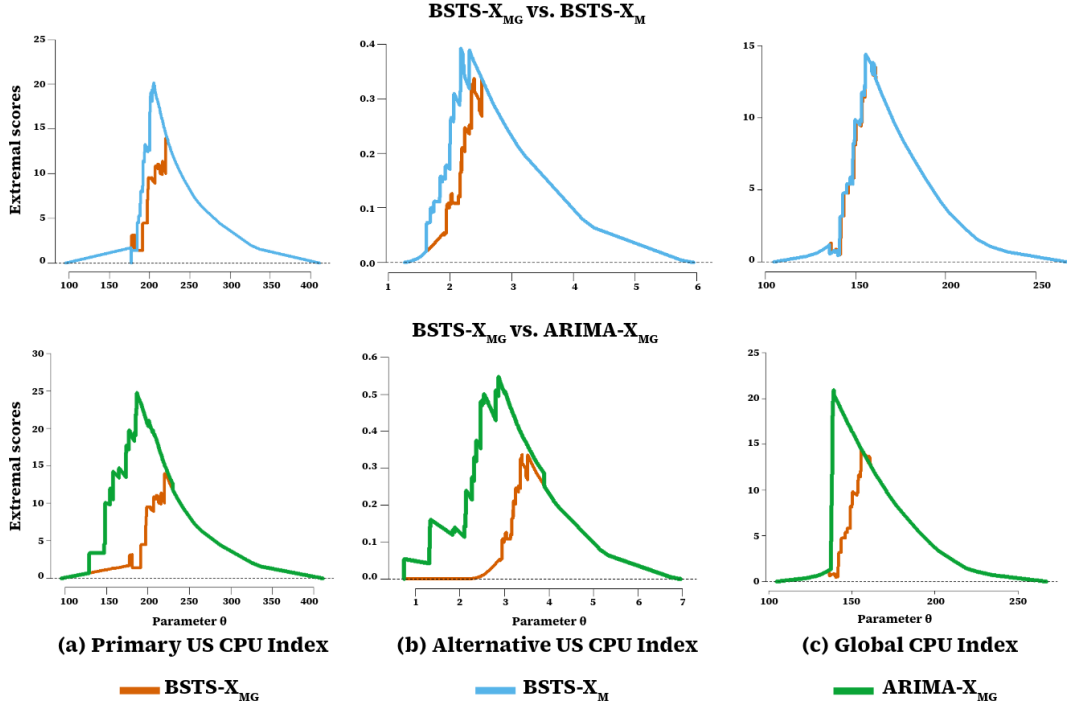


Figure 4: Murphy diagrams of BSTS- X_{MG} with baselines (BSTS- X_M (top) and ARIMA- X_{MG} (bottom)) for the 24-month-ahead forecasts for the (a) primary US, (b) alternative US, and (c) Global CPU indices. The parameter θ represents the shape parameter as defined in Eqn. (2). Lower scores indicate better performance.

quently, the use of time-invariant coefficients in BSTS- X_{MG} is empirically justified and supports informed climate policy planning and investment decisions without introducing unnecessary model complexity.

6.6. Impulse Response Analysis

To empirically validate the theoretical links discussed in Sections 2 and 4.2 and further enhance the economic intuition, this section examines the responses of the primary US CPU index to innovations in key macroeconomic and financial cycle variables. These innovations correspond to one-standard-deviation forecast errors from the estimated model rather than identified structural shocks. The impulse response analysis is conducted using the local projections method of [52], which is well-suited in this context due to its resilience to model misspecification and its flexibility in estimating dynamic effects without imposing restrictive assumptions often associated with vector autoregression (VAR) models. Given the structural uncertainty and high dimensionality associated with the determinants of the CPU index, the local projection approach offers a transparent framework for quantifying how unexpected movements, such as an increase in unemployment or shifts in credit markets, impact CPU across various time horizons. This approach is particularly beneficial in climate policy-related research, where grasping the timing, volatility, and persistence of policy uncertainty is essential for crafting adaptive and forward-thinking strategies. Therefore, this analysis provides deeper insights into the dynamic transmission processes between macroeconomic and financial cycle factors and the CPU index.

The impulse response analysis focuses on sixteen variables: business confidence index (BCI), composite leading indicator (CLI), real S&P500 index growth (SP500), cyclically adjusted price-to-earnings ratio (CAP/Earnings), real credit growth (CRED), credit-to-GDP ratio (CRED/GDP), house price index (HPI), cyclically adjusted price-to-rent ratio (CAP/Rent), household real mortgage debt growth (Mortgage), household mortgage-to-income ratio (Mortgage/Income), private residential fixed investment-to-GDP ratio (PRFI/GDP), personal interest payments-to-income ratio (PIP/Income), unemployment rate (Unemployment Rate), total housing starts (HOUST), real personal

Table 9: Evaluation of BSTS- X_{MG} models with time-invariant and time-varying regression coefficients (BSTS- X_{MG}^{TI} and BSTS- X_{MG}^{TV} , respectively) across all forecast horizons and CPU indices using macro-financial variables and Google Trends indicators. The **best** results are highlighted.

Horizon	Metric	CPU Index					
		Primary (US)		Alternative (US)		Global	
		BSTS- X_{MG}^{TI}	BSTS- X_{MG}^{TV}	BSTS- X_{MG}^{TI}	BSTS- X_{MG}^{TV}	BSTS- X_{MG}^{TI}	BSTS- X_{MG}^{TV}
3	MAPE	4.708	26.641	23.856	46.761	18.107	30.275
	SMAPE	4.598	24.641	22.791	32.492	16.070	26.014
	MAE	10.568	59.926	0.428	0.727	26.115	45.461
	MASE	1.817	10.303	0.854	1.450	1.0102	1.759
	RMSE	10.655	64.737	0.435	0.943	30.484	46.470
6	MAPE	6.029	23.638	23.627	22.231	16.176	18.171
	SMAPE	6.343	27.664	23.954	22.034	16.179	20.728
	MAE	15.572	57.833	0.469	0.411	28.673	34.636
	MASE	0.530	1.968	0.890	0.779	1.024	1.237
	RMSE	24.201	68.115	0.506	0.483	32.601	42.796
12	MAPE	11.345	32.280	43.469	79.300	15.553	12.755
	SMAPE	12.133	42.321	44.755	113.716	14.596	13.383
	MAE	29.361	79.859	0.928	1.849	25.012	22.110
	MASE	0.842	2.289	1.224	2.438	1.181	1.044
	RMSE	44.153	100.536	1.140	2.345	28.018	27.415
24	MAPE	18.194	33.267	33.092	110.307	18.247	29.277
	SMAPE	19.182	39.950	36.085	155.571	20.305	36.051
	MAE	44.670	79.877	1.028	3.000	35.001	55.830
	MASE	0.728	1.301	0.844	2.464	0.910	1.452
	RMSE	66.440	98.975	1.416	3.381	44.656	66.796

consumption expenditures (DPCERA3M086SBEA), and new private housing permits in the northeastern US (PERMITNE). These variables represent the widest spectrum of the overall aggregate macroeconomy, covering major sectors, such as labor, credit, housing, consumption, and financial markets, to provide exploratory insights into how broader macroeconomic conditions influence the CPU index.

This analysis employs the local projections methodology on the training sample of monthly data spanning April 1987 through June 2021 to examine the dynamic impact of financial and macroeconomic innovations on the CPU index. The estimation of the impulse response functions follows the local projections methodology originally developed by [52], and computationally implemented by the `lpirfs` package in **R** [2]. This approach fundamentally differs from the VAR method by employing direct sequential regressions on future realizations of the dependent variable, thereby preventing the necessity to specify and invert a complete multivariate dynamic system [52]. This study employs linear local projections estimated via the `lp_lin` function with the following specifications: a maximum lag length of 12 months determined by the Bayesian Information Criterion (`max-lags = 12`), a linear time trend (`trend = 1`), innovations standardized to one standard deviation (`shock-type = 0`), and 95% confidence intervals computed using heteroskedasticity and autocorrelation-robust Newey-West [76] standard errors (`confint = 1.96, use-nw = TRUE`). The analysis estimates impulse response functions across a 24-month-ahead horizon (`hor = 24`). In this study, the CPU index measures the degree of uncertainty in climate-related policy, with higher values indicating greater uncertainty. This is essential for interpreting the impulse response results. A positive impulse response signifies an increase in CPU, while a negative response represents a reduction in uncertainty.

Fig. 5 illustrates the dynamic responses of the CPU index to innovations in macroeconomic and financial cycle variables across a 24-month-ahead horizon. The impulse response analysis shows that the variables have economically meaningful and statistically significant effects on the CPU index, either positively or negatively. Among the variables that have positive influences, CAP/Earnings exhibits a consistently positive effect over the 24-month-ahead horizon, albeit with some fluctuations, indicating a persistent and substantial relationship in which equity market overvaluation increases CPU. A positive relation between CAP/Earnings and CPU suggests that when the markets have high valuations, any regulation change, including climate-related policies such as an increase in environmental taxes or upgradation of production facilities, can increase the companies' costs and reduce their profitability. Reduced earnings in the period of overvalued financial markets lead to a sharp market correction. Hence, during market overvaluation, the investors can be very sensitive to changes in climate-related regulatory policies, thereby increasing the perceived uncertainty. The impulse response of CPU to PIP/Income is also positive. This positive

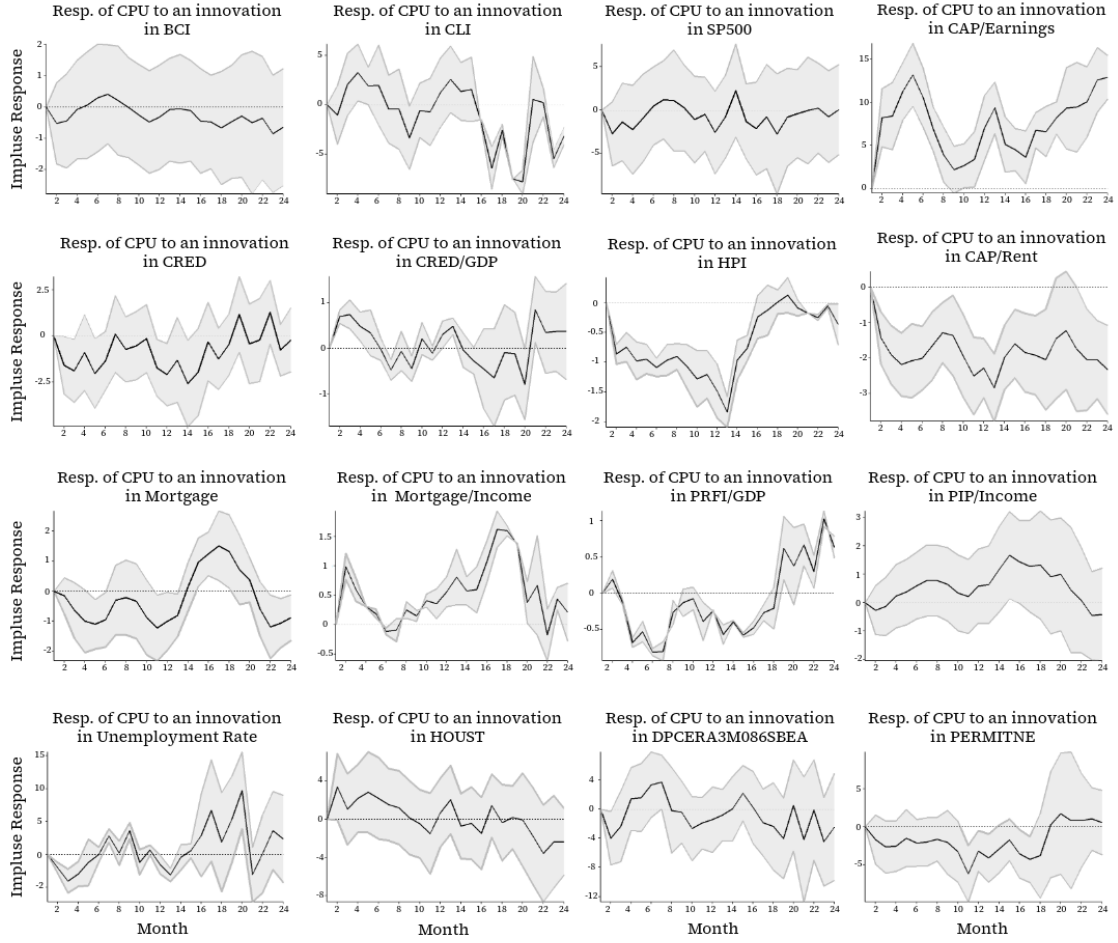


Figure 5: Impulse response functions generated via the local projections method, quantifying the CPU index’s dynamic reactions to one-standard-deviation innovations in macroeconomic and financial cycle variables. The reaction is represented by the solid black line, and the 95% confidence intervals are represented by the gray shaded regions. The dashed black line displays the zero line. The sample period runs from April 1987 to June 2021.

relationship implies that when households face higher interest payments relative to their income to service debt, they become more sensitive to regulatory changes, including those related to climate policy. This reflects a tension between the increased financial vulnerability of individual households and the perceived cost of implementing climate policy regulations. Similarly, Mortgage/Income exhibits a predominantly positive effect over the 24-month-ahead horizon, indicating that higher household debt burdens amplify financial vulnerability and public sensitivity to climate-related regulatory changes. In addition, CRED/GDP shows a predominantly positive effect, indicating a sustained relationship between systemic leverage and CPU. An elevated level of credit relative to GDP heightens financial vulnerability, which may discourage policymakers from implementing substantial policy changes that could destabilize corporate financial situations [6]. Adoption and compliance with new climate regulations typically require significant business investment. In an environment of excessive credit growth relative to GDP, central banks may implement stricter macroprudential policies to contain systemic risk. Such tightening can limit firms’ capacity to invest in compliance with climate regulations, thereby heightening CPU.

Further supporting the sensitivity of CPU to cyclical macroeconomic conditions is its mostly positive response to the unemployment rate. When the unemployment rate increases, the focus shifts from environmental concerns to basic survival needs. This again makes households reluctant to comply with any new environmental policies, thereby making the introduction and implementation of any changes to climate policy regulation very difficult and politically

sensitive. Lastly, we observe a positive response with PRFI/GDP, though the effect occurs in the first three months and reemerges during the final six months of the 24-month horizon. A greater PRFI/GDP indicates a rise in residential construction, which may lead to increased environmental consequences such as elevated energy consumption, land development, and construction-related emissions. This may drive policymakers to propose stricter climate regulations to alleviate the threats to environmental or climatic degradation. The policies may include stricter emission controls, increased taxes, or changes in the building standards. This expectation of any forthcoming rigorous and stringent policies can increase uncertainty surrounding climate policy, regarding their timing and intensity, thereby positively influencing the CPU index [28].

Now we shift our focus to the variables that exert a negative and statistically significant influence on the CPU index. CAP/Rent depicts an intensely negative and consistent impact throughout the 24-month-ahead horizon. The economic intuition behind this effect's sustained nature is that an increase in property prices relative to rental income reflects an increase in the net worth of the homeowners and creates a wealth effect. An increase in the real estate asset price can be linked with reduced uncertainty and increased investor confidence, making them more optimistic about the future economic outlook. Increased optimism about the future economic outlook, coupled with increased wealth, makes individuals and businesses more adaptive to climate change policies. Similarly, HPI demonstrates a negative and statistically significant response. The negative response suggests that increasing house prices signal economic stability and rising housing demand. This improved economic stability may reduce CPU as people are expected to have a higher disposable income to comply with new environmental or climate regulations. Hence, policymakers experience both lower resistance and political pressure to alter existing environmental policies [78; 21]. Moreover, Mortgage shows a predominantly negative impact on CPU over the 24-month-ahead horizon, as stable financing conditions reduce household financial stress and dampen sensitivity to climate-related regulatory changes. In addition, PERMITNE exhibits a largely negative effect, suggesting that stronger forward-looking construction activity signals macroeconomic resilience and greater household and firm adaptability to climate regulations. Similarly, HOUST shows a negative response despite an initially positive effect, indicating that while short-run increases in construction activity may raise regulatory concerns, sustained housing expansion ultimately reduces uncertainty as income and investment conditions improve [28].

The negative response of the CPU index to CRED can be attributed to the fact that business cycles alternative between economic recovery and recession. When the economy enters the recovery phase following a recession or stagnation, an initial wave of credit growth typically emerges, driven by rising investment and employment opportunities at the start of the new cycle. This period is often marked by robust corporate profits and growing household incomes, thereby creating a favorable environment for policymakers to simultaneously introduce and implement ambitious climate-related policies. However, when credit growth exceeds the growth rate of economic output, the resulting increase in credit can heighten climate-related uncertainties, as previously discussed in the case of CRED/GDP. The business confidence measures, BCI and CLI, exhibit predominantly negative responses over the 24-month-ahead horizon, indicating that stronger forward-looking economic expectations can reduce CPU, although its response to CLI fluctuates, reflecting its sensitivity to cyclical conditions [103]. Similarly, DPCERA3M086SBEA exhibits a mostly negative effect, suggesting that stronger consumption reflects economic expansion and public confidence, thereby creating political space for the implementation of climate policies with lower perceived uncertainty [102]. Regarding the S&P 500 index, it demonstrates a negative and statistically significant impact on CPU. S&P 500 acts as a sentiment barometer for the aggregate macroeconomy, which influences the perceived viability of climate-friendly and environmental investments. Rising stock prices in equity markets lead to increased wealth in the hands of investors. The positive wealth effect creates positive sentiment about the economy among investors. This forward-looking optimism enhances the commitment of households and businesses towards adherence to any new changes in environmental and climate change regulations. Such enhanced commitment and positive economic outlook give an opportunity to policymakers to pursue and implement new climate change policies. The opposite scenario occurs during a recession-driven bear market when negative forward-looking behaviour makes it difficult for policymakers to implement stricter climate policies [56; 4].

The impulse response analysis results indicate that the effects of macro-financial conditions on CPU are not only statistically significant but also economically meaningful and persistent over time. Periods characterized by financial stability, rising asset prices, and strong confidence provide governments with greater political and fiscal capacity to sustain long-term climate commitments. Favorable economic conditions create a buffer that facilitates credible and consistent policy communication, as households and firms are better positioned to absorb the adjustment costs associated with the green transition. By contrast, during episodes of financial stress or economic contraction, heightened

financial vulnerability and weakened confidence constrain policymakers’ scope for action, shifting priorities toward short-term stabilization. Consequently, environmental commitments are more likely to be delayed, diluted, or re-framed as governments adopt a reactive stance to mitigate immediate economic pressures. This cyclical reorientation of policy objectives leads to inconsistencies in climate policy direction, which manifests as pronounced increases in CPU. These patterns underscore that CPU is closely linked to the underlying condition of the state of the economy.

6.7. Economic Interpretation of Feature Importance Plot

In Sections 6.3 and 6.4, we highlighted the superior performance of the BSTS model compared to both classical and modern forecasting architectures. In this section, we provide insight into the superior performance of the BSTS model by examining its variable selection mechanism. For interpretability, we focus on the macroeconomic and financial cycle variables, excluding the Google Trends indicators. Nonetheless, their relevance remains clear from the preceding results and Fig. 2, where the time series of several climate-related search terms closely mirror the evolution of CPU, underscoring their complementary role in capturing public sentiment surrounding CPU. To examine whether the variables selected by the BSTS model align with economic theory in Section 4.2 and empirical impulse response analysis in Section 6.6, we analyze the feature importance plot generated by the BSTS model over the 24-month forecast horizon. Fig. 6 highlights the variables with the highest inclusion probabilities, reflecting broad sectors of the economy, such as financial markets, housing, labor, and economic sentiment, that are theoretically linked to CPU.

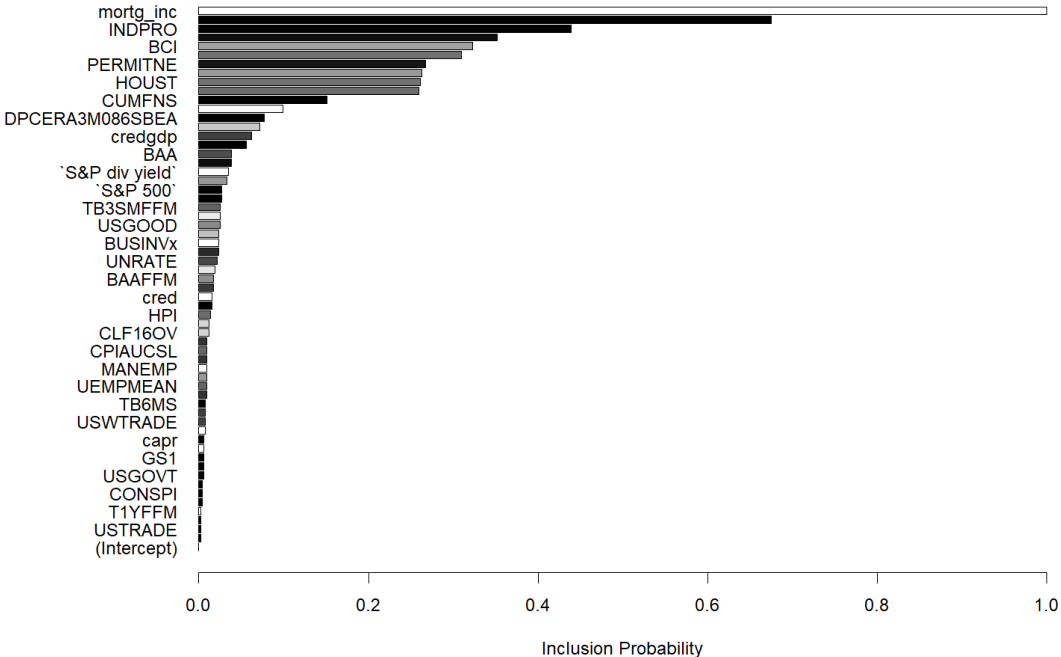


Figure 6: Inclusion probabilities of variables selected by the BSTS model over a 24-month-ahead forecast horizon. The plot reflects the relative importance of each variable in contributing to the model’s predictive accuracy, with higher probabilities indicating greater explanatory relevance. The full form of the variables displayed on the y-axis is detailed in Table A.10

The top ten variables selected by the model, as illustrated in Fig. 6, exhibit the highest inclusion probabilities. Importantly, these variables are consistent with economic theory and with the factors previously identified as significant determinants of CPU in Sections 4.2 and 6.6. At the top of the list is the mortgage-to-income ratio (mortg_inc), which captures household financial vulnerability to interest rate changes when central banks increase rates. Higher mortgage burdens reduce disposable income, thereby heightening public resistance to policies that might increase living costs. Such resistance, in turn, can pressure policymakers to postpone or soften environmental initiatives. The industrial production index (INDPRO) monitors real economic output across major industrial production sectors of the US and plays an important role due to its direct correlation with energy consumption and emissions. Fluctuations in industrial activity can deter firms from adopting new environmental regulations, complicating policymakers’

efforts to balance economic growth with environmental sustainability. Similarly, the business confidence index (BCI) captures firms' expectations about future economic conditions and investment decisions, including their willingness to commit resources toward compliance with green policies [103]. Together, INDPRO and BCI represent the current and forward-looking dimensions of business sector performance and are tied to CPU.

The model also gives high inclusion probabilities to housing sector indicators, such as new private housing permits in the northeastern US (PERMITNE) and total housing starts (HOUST). Their inclusion is consistent with economic theory and earlier findings in this study, confirming the macroeconomic relevance of the housing sector in shaping the CPU index. High values of PERMITNE and HOUST reflect a robust construction sector and signal overall economic vitality. In such periods of optimism, governments face fewer constraints in implementing long-term climate policies, as households are more financially secure and more receptive to adopting climate-friendly technologies, such as energy-efficient installations in new homes. Conversely, a decline in housing permits and new home construction signals economic weakness or stagnation. Under such conditions, policymakers may delay or soften environmental regulations to avoid further straining the housing and real estate sector. As highlighted by [28], stringent climate regulations can amplify vulnerabilities in an already fragile housing market, underscoring the delicate balance policymakers must strike between environmental and macroeconomic stability. The manufacturing capacity utilization (CUMFNS) measures the extent to which existing productive capacity is being employed. High utilization rates generate resource constraints and inflationary pressures, prompting interest rate hikes, whereas low utilization motivates monetary easing to stimulate growth. Lower interest rates, in turn, accelerate the transition toward clean energy since lowering financing costs enables firms to invest more readily in environmentally sustainable technologies. However, the inclusion probability of CUMFNS is notably lower than that of PERMITNE and HOUST, which is consistent with our earlier discussion, in Section 4.2, that housing indicators exert a stronger influence on CPU dynamics than sector-specific production measures.

The inclusion of real personal consumption expenditures (DPCERA3M086SBEA) and the credit-to-GDP ratio (credgdp) further confirms the consistency of the model's variable selection with economic reasoning. As discussed earlier, both variables play a central role in shaping macro-financial dynamics and, consequently, CPU. Consumer spending is a key driver of economic activity in the US, reflecting household confidence and overall economic health. A sustained rise in real personal consumption signals economic prosperity, enabling governments to pursue more ambitious climate actions. Conversely, a contraction in consumption coincides with heightened economic uncertainty, which can lead to delays or moderation in climate policy initiatives [102]. Similarly, the credit-to-GDP ratio captures the level of financial leverage within the economy. Elevated levels increase systemic vulnerability, making policymakers more cautious about introducing policies that could disrupt credit markets. During such periods, central banks tighten macro-prudential regulations to contain financial risks, which indirectly slows the pace of climate policy implementation by limiting investment and credit availability for green projects. The indicators S&P 500 dividend yield and Moody's Seasoned Baa Corporate Bond Yield (BAA) capture capital market conditions, credit risk, and market sentiment, all of which are crucial in shaping CPU. Increases in bond yields or high dividend yields signal investor caution and a shift toward risk-averse behavior, particularly in capital-intensive and regulated industries. Such caution can heighten market sensitivity to policy changes, leading investors and firms to delay climate-related investments or push back against stringent policy measures.

The ten factors identified by the model span broad dimensions of the economy, capturing sectoral exposure to policy risk and macro-financial stability [6; 39]. All of these factors have been found to have a significant impact on CPU. This coherence with economic theory provides a strong justification for the model's superior predictive performance, as it successfully isolates the most economically relevant predictors of CPU. We also observe that several variables previously identified as theoretically relevant to CPU appear in Fig. 6 with smaller inclusion probabilities. These include S&P 500 index, unemployment rate (UNRATE), credit growth (cred), real house price growth (HPI), and the cyclically adjusted price-to-rent ratio (capr). Their limited inclusion probabilities suggest that while they contain information related to CPU, their explanatory contribution is largely captured by more dominant macro-financial variables already included in the model, such as credit-to-GDP ratio, INDPRO, and the housing indicators (PERMITNE and HOUST). It is worth noting that, despite their intuitive relevance, sector-specific variables such as mining employment do not appear among the top predictors in Fig. 6. This outcome is economically consistent with how CPU propagates through the economy. CPU is not confined to specific industries but reflects broader expectations, confidence, and investment behavior across households, firms, and financial markets. Thus, aggregate indicators, such as housing activity, credit conditions, and financial market sentiment, capture the nature of policy uncertainty more effectively than sectoral metrics in individual industries.

Interestingly, other related variables, such as the 3-month treasury bill minus federal funds rate (TB3SMFFM), all employees in goods-producing industries (USGOOD), and the consumer price index (CPI) for all urban consumers (CPIAUCSL), appear in the feature importance plot with small but non-zero inclusion probabilities. These can be interpreted as complementary measures that reflect similar underlying mechanisms to those captured by the earlier-identified but weakly included variables. For instance, treasury spreads and short-term interest rate differentials serve as proxies for financial conditions and market expectations, linking indirectly to credit growth and equity market sentiment. Likewise, variables such as manufacturing employment (MANEMP), wholesale and retail trade employment (USWTRADE and USTRADE), and the civilian labor force level (CLF16OV) capture aggregate labor market dynamics that are closely related to the unemployment rate, whereas CPI provides an alternative channel for capturing household purchasing power and cost-of-living pressures that affect public support for climate policies. In contrast, some variables we initially considered relevant, such as the composite leading indicator, private residential fixed investment-to-GDP ratio, and personal interest payments-to-income ratio, do not appear in Fig. 6. This likely reflects multicollinearity, as their effects are proxied by broader housing and credit indicators that provide more stable predictive signals. Overall, this analysis confirms that the model’s variable selection mechanism identifies predictors consistent with both economic theory and our empirical findings, with inclusion probabilities clearly differentiating the primary drivers of CPU from secondary contributors.

6.8. Uncertainty Quantification using Credible Intervals

Finally, we aim to quantify the uncertainty associated with the BSTS forecasts by analyzing the model’s credible intervals. In Bayesian statistics, a credible interval is the range within which a forecast lies with a certain probability, given the posterior distribution. Unlike frequentist confidence intervals, which are based on hypothetical repeated sampling, credible intervals are directly derived from the posterior distribution, incorporating both prior knowledge and observed data. Let $y_{1:T}$ represent the observed time series up to time T . The predictive distribution for y_{T+h} at horizon h conditional on the past observations $y_{1:T}$ is expressed as:

$$p(y_{T+h} | y_{1:T}) = \int p(y_{T+h} | \theta, y_{1:T}) p(\theta | y_{1:T}) d\theta,$$

where $p(y_{T+h} | \theta, y_{1:T})$ is the likelihood of the future observation given model parameters θ , and $p(\theta | y_{1:T})$ is the posterior distribution of the parameters after observing the data $y_{1:T}$. This integration captures both the uncertainty in the future outcomes and the model parameters.

The $100(1 - \alpha)\%$ credible interval for the forecast at $T + h$ is defined as the interval within which y_{T+h} lies with posterior probability $1 - \alpha$, such that $P(L_{T+h} \leq y_{T+h} \leq U_{T+h} | y_{1:T}) = 1 - \alpha$, where L_{T+h} and U_{T+h} denote the lower and upper bounds of the credible interval, respectively. These bounds correspond to the quantiles of the posterior predictive distribution, expressed as $L_{T+h} = F^{-1}(\alpha/2)$ and $U_{T+h} = F^{-1}(1 - \alpha/2)$, with $F^{-1}(\cdot)$ denoting the inverse cumulative distribution function of the predictive distribution. In practice, since the posterior distribution is usually approximated via Monte Carlo sampling, the credible interval is obtained from the empirical quantiles of the simulated forecasts as $L_{T+h} = \hat{y}_{T+h}^{(m_{\alpha/2})}$ and $U_{T+h} = \hat{y}_{T+h}^{(m_{1-\alpha/2})}$, where $\hat{y}_{T+h}^{(m)}$ denotes the forecast from the m -th draw, and $m_{\alpha/2}$ and $m_{1-\alpha/2}$ correspond to the empirical quantiles of the posterior sample at the $\alpha/2$ and $1 - \alpha/2$ levels, respectively [79].

Fig. 7 presents the 6-month-ahead forecasts for the CPU index across the three series produced by the BSTS- X_{MG} model. The left panel displays the training series alongside the fitted values, illustrating the model’s strong in-sample fit and its ability to replicate the historical dynamics of the CPU index. The right panel depicts the point forecasts and the 95% credible intervals of the BSTS- X_{MG} together with the point forecasts from ARIMA- X_{MG} . Although ARIMA- X_{MG} demonstrates strong performance, it fails to adequately capture the volatility observed in the CPU index during the test period. This limited responsiveness to evolving patterns underscores its weakness for policy uncertainty forecasting. In contrast, BSTS- X_{MG} achieves closer alignment with the ground truth and demonstrates superior adaptability to the series’ dynamic behavior. This adaptability is further strengthened by the model’s explicit quantification of forecast uncertainty through credible intervals derived directly from the posterior predictive distribution. These intervals provide a probabilistic range within which future CPU values are expected to lie, reflecting the model’s ability to realistically account for substantial uncertainty in climate-related policy dynamics. The credible intervals enable policymakers to better understand the range of plausible future outcomes and to plan

accordingly under uncertainty, thus making BSTS a more informative and robust forecasting framework. Overall, the capacity of BSTS to adapt to changing trends while rigorously quantifying uncertainty establishes it as a reliable tool for forecasting policy-sensitive and volatile series such as the CPU index.

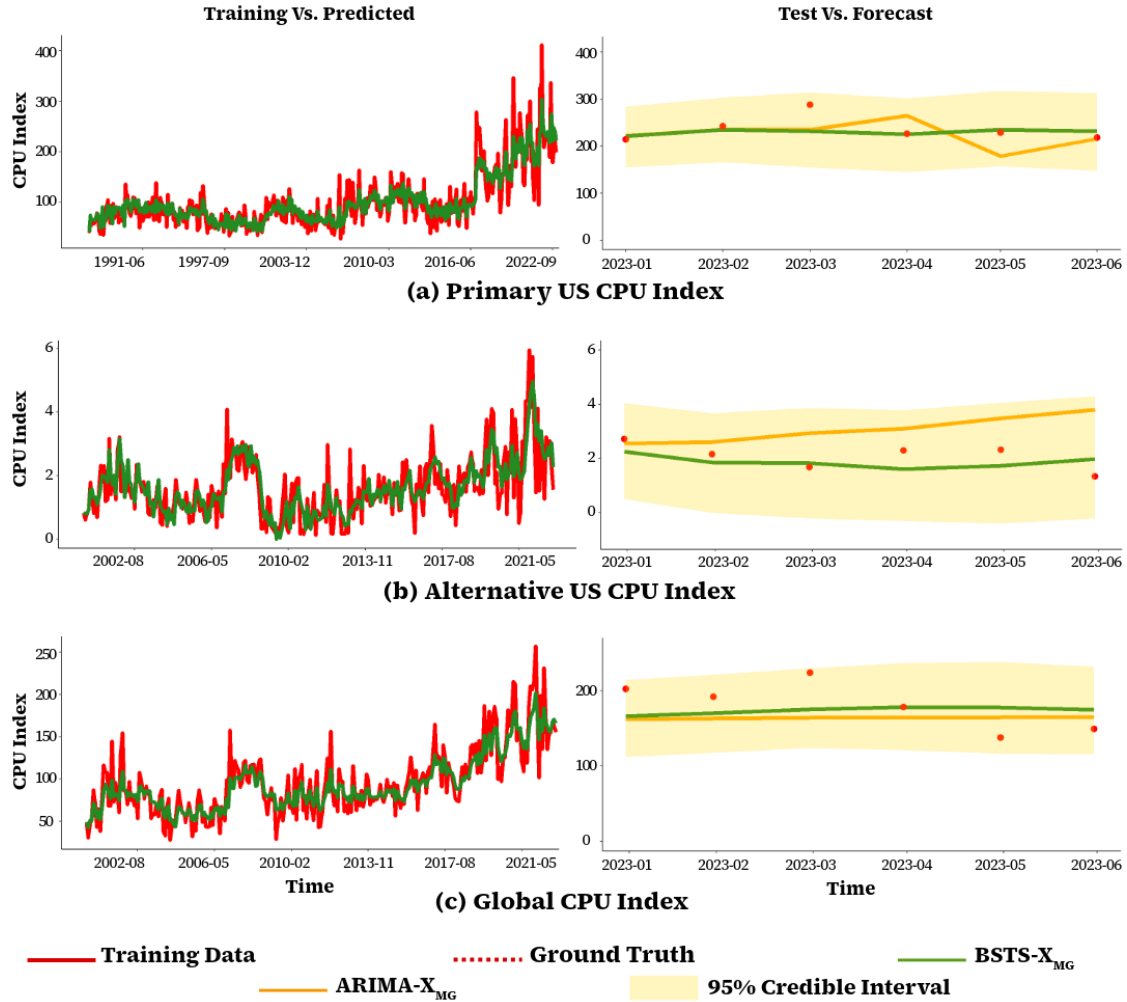


Figure 7: Visualization of the ground truth (red), fitted values and forecasts of the BSTS- X_{MG} model (green), forecasts of ARIMA- X_{MG} (orange), and the credible intervals generated by BSTS (yellow shaded) for the 6-month holdout period of the (a) primary US, (b) alternative US, and (c) Global CPU series. The plot on the left displays the training data along with the fitted values of BSTS- X_{MG} . The plot on the right presents the semi-long-term forecasts shown as both point estimates and credible intervals.

7. Policy Implication

This study uncovers a complex relationship between macro-financial conditions and the dynamics of the CPU index, with clear differences in the relative influence of key predictors. The most influential factors are household financial vulnerability (mortgage-to-income ratio), business confidence (BCI), and housing activity (PERMITNE, HOUST). High mortgage burdens signal financial strain, which can increase public resistance to policies perceived as raising living costs, thereby amplifying CPU. Forward-looking indicators such as BCI capture expected business and household sentiment; elevated confidence tends to reduce CPU by fostering investment and regulatory compliance, while low confidence signals economic stress, leading governments to prioritize short-term recovery over long-term

climate goals. Housing indicators, including PERMITNE and HOUST, reflect broader economic vitality; strong activity provides policymakers more latitude to implement stringent climate measures, whereas downturns constrain policy action [28].

Secondary predictors provide additional, though less dominant, information. These include industrial production, manufacturing capacity utilization, the real personal consumption, credit-to-GDP ratio, and market valuations such as S&P 500 dividend yields and Moody’s Baa bond yields. For example, higher asset prices or home price indices are generally associated with lower CPU, as stronger asset performance fosters optimism and reduces perceived policy risk. Conversely, elevated financial leverage, overvalued markets, or constrained credit conditions increase uncertainty by heightening sensitivity to regulatory changes because such monetary tightening can deter firms and households from investing in green technologies, thereby increasing uncertainty about future climate policy directions. Other variables, including short-term treasury spreads, labor market indicators, CPI, and sector-specific employment measures, provide complementary information but exert smaller effects. Their lower inclusion probabilities, as depicted in Fig 6, indicate that their contributions are largely captured by dominant macro-financial variables such as housing, credit, and confidence indicators.

Dynamic local projection analysis further quantifies these associations over time. Higher cyclically adjusted price-to-earnings, household debt burdens (mortgage-to-income, personal interest payments-to-income), and credit-to-GDP ratios are associated with increases in CPU, reflecting greater sensitivity to regulatory changes during periods of financial vulnerability or overvalued markets. In contrast, stronger housing activity (PERMITNE, HOUST), rising property prices (HPI, cyclically adjusted price-to-rent ratio), elevated business confidence (BCI, CLI), personal consumption growth, and equity prices are associated with reductions in CPU, indicating that healthier macro-financial conditions facilitate policy implementation. These patterns confirm that CPU intensifies during downturns and moderates during expansions, consistent with prior evidence linking recessions to weaker environmental policy commitment [51]. Public sentiment, captured through Google Trends indicators, also plays an equally important role. Search intensity for climate-related terms provides a quantifiable proxy for societal attention and concern. These sentiment-based indicators reflect early shifts in collective awareness that often precede policy debates or legislative actions. Their inclusion significantly improved long-term forecast accuracy, underscoring the value of integrating behavioral dimensions into traditional economic forecasting frameworks.

Our results indicate that CPU is not only a phenomenon dependent on macroeconomic cycles but also a governance challenge at the implementation level. The strong predictive power of macroeconomic variables suggests that rigid regulatory interventions may be ineffective during recessions. Instead, climate policies should be adaptive, incorporating phased compliance, conditional enforcement triggers, and pre-specified review clauses. These measures should preserve long-term climate commitments, while allowing short-term flexibility in execution. Such features will enhance policy credibility and reduce the risk of abrupt reversals. This approach directly addresses uncertainty faced by regulatory bodies, firms, and individuals, and mitigates inconsistencies in policy enforcement during periods of economic stress.

Our findings further demonstrate that effective implementation of environmental policies requires coordination from entities beyond environmental agencies alone. The significant influence of housing, credit, and household financial stress variables on CPU suggests that climate policy implementation depends on broader economic governance structures. Consequently, climate regulations will be more effective when they are coordinated with financial regulation, housing policy, and fiscal support mechanisms. For example, authorities should design interest rate-sensitive policy instruments that give more robust subsidies or low-interest financing for green technologies when market credit conditions tighten, thereby maintaining steady progress even during tight liquidity conditions. The adaptability of households and firms to environmental mandates can be further increased if they are integrated with green finance instruments, targeted subsidies, or credit guarantees. In economic downturns, instead of rolling back climate regulations, green fiscal stimuli should be provided. These green stimuli will motivate firms to support continued investment in environmental technologies, preventing a “lost decade” for climate action. Such integration of climate policies with macroeconomic frameworks can substantially lower the adjustment costs.

This study underscores the importance of expectation management and information governance in mitigating CPU. The significant role of sentiment-based indicators implies that uncertainty reflects ambiguity about policy direction and its credibility rather than the absence of policy. Hence, it is imperative for environmental authorities to address policy uncertainty with transparent communication strategies, which include providing forward guidance

on regulatory pathways, predictable rulemaking schedules, and clear signaling of long-term policy continuity. Such measures are indispensable for strengthening institutional trust among the stakeholders and reducing informational frictions, which is critical for effective policy implementation in politically and economically volatile environments.

Finally, the probabilistic forecasting framework employed in this study provides a practical tool for risk-aware environmental planning. Rather than relying solely on deterministic projections, environmental managers can leverage forecast distributions of CPU to identify periods of heightened implementation risk. Accordingly, they can design contingency measures to enhance the implementation of climate-related regulations. Integrating uncertainty quantification into policy evaluation enables regulators to anticipate challenges in implementing climate policies, prioritize interventions, and sustain climate objectives across economic cycles. This integrated approach shifts environmental management from a reactive to a forward-looking, robust governance framework that explicitly accounts for economic and political uncertainty.

8. Conclusion

This study provides the first systematic attempt to forecast US and global CPU, shifting attention from its consequences to the identification of its underlying predictors. To this end, we integrate four empirical screening techniques to rigorously identify macro-financial variables most strongly associated with CPU. The selected predictors are not only statistically significant but also theoretically grounded, aligning with economic reasoning regarding household financial vulnerability, business confidence, and housing activity, among other channels. To quantify the dynamic influence of these predictors on CPU, we employ local projection impulse response analysis. This approach reveals that increases in asset prices, business confidence, and consumption reduce CPU, whereas elevated financial leverage, high debt burdens, or overvalued markets amplify uncertainty. These results highlight the cyclical nature of CPU, which intensifies during downturns and moderates during expansions, and demonstrate how macro-financial conditions propagate through the economy to influence CPU over time.

Recognizing that CPU also reflects public perception, we incorporate sentiment-based indicators derived from Google Trends. These measures capture early shifts in societal attention to climate policies and empirically improve forecast accuracy, underscoring the value of integrating behavioral dimensions alongside traditional economic indicators. Using these variables, we forecast both US and Global CPU indices, providing a comprehensive assessment of predictive performance and model robustness across indices. Our extensive experiments demonstrate that BSTS with time-invariant regression coefficients achieves the highest forecasting accuracy for all CPU indices. Importantly, this analysis demonstrates that BSTS's forecasting accuracy is not coincidental but stems from its principled selection of variables whose impacts are consistent with economic theory and validated empirically through dynamic response analysis. This link between theory and predictive power is illustrated in the feature importance plot, which identifies household financial vulnerability (mortgage-to-income ratio), business confidence (BCI), and housing activity (PERMITNE, HOUST) as the variables with the largest dynamic impacts on CPU, while secondary predictors, such as industrial production, credit-to-GDP ratios, and market valuations, provide complementary information that captures how uncertainty propagates through macro-financial channels.

From a policy perspective, these findings indicate that rigid interventions may be less effective during economic downturns. Climate policies should therefore be adaptive, incorporating phased compliance, conditional enforcement, and pre-specified review mechanisms to balance long-term objectives with short-term flexibility. Implementation is most effective when coordinated across housing, credit, and fiscal policy, and supported by green financing instruments and targeted fiscal measures to sustain progress under economic stress. Clear communication, forward guidance, and predictable rulemaking enhance institutional trust and reduce informational frictions, helping stabilize CPU. Finally, probabilistic forecasts of CPU allow regulators to anticipate high-risk periods, prioritize interventions, and maintain climate objectives consistently across economic cycles. Overall, this study demonstrates that accurate CPU forecasting requires a careful combination of rigorous variable selection, theoretical validation, and dynamic quantification of predictor effects. By uncovering the key predictors of CPU and integrating sentiment-based indicators, we provide the first empirically validated, theoretically grounded, and robust approach to anticipating CPU. These findings underscore the importance of aligning forecasting methodologies with economic theory, showing that predictive success is inseparable from understanding the underlying mechanisms driving uncertainty.

One limitation of this study concerns the geographic scope of the analysis. Although both US and Global CPU indices are analyzed, the findings remain largely US-centric, which may limit their applicability to regions with different macroeconomic structures, financial systems, or climate policy environments. Expanding the study to incorporate additional regional or country-level indicators could further validate the robustness and applicability of the results and provide a more comprehensive understanding of the predictors of CPU worldwide. Another limitation lies in not incorporating political or environmental factors that may also play a role in shaping CPU. For example, political uncertainty, such as election cycles or government transitions, may influence CPU, as it often coincides with fluctuations in consumer confidence and broader economic uncertainty. Similarly, environmental factors, including extreme weather events, pollution, wildfires, and carbon emission metrics, could exert substantial influence on policy uncertainty dynamics. Future research could incorporate such factors to allow for a more comprehensive assessment of the relative contributions of macro-financial, political, and environmental predictors of CPU.

Code and Data Availability

The primary US CPU index used in this study was obtained from the Economic Policy Uncertainty website: https://www.policyuncertainty.com/climate_uncertainty.html. The alternative US and Global CPU indices used in this study were sourced from the China Energy and Environmental Policy Research Center Network website: <http://www.cnefn.com/data/download/climate-risk-database>. For transparency, all datasets, including the statistically significant macro-financial predictors and Google Trends indicators, as well as the code necessary to reproduce the findings presented in this paper are made available on Github: https://github.com/Donia-212/Climate_Policy_Uncertainty_Forecasting.

Acknowledgement

The authors would like to acknowledge the Associate Editor and two experienced reviewers for insightful suggestions that improved the paper. The authors want to thank Madhurima Panja of Sorbonne University Abu Dhabi for the discussion and help with the graphics presented in this manuscript.

References

- [1] Tomiwa Sunday Adebayo, Mustafa Tevfik Kartal, Mehmet Ağa, and Mamdouh Abdulaziz Saleh Al-Faryan. Role of country risks and renewable energy consumption on environmental quality: Evidence from MINT countries. *Journal of Environmental Management*, 327:116884, 2023.
- [2] Philipp Adämmer. lpirfs: An R Package to Estimate Impulse Response Functions by Local Projections. *The R Journal*, 11:421–438, 2019.
- [3] T. Akan. The impact of monetary policy on climate change through the mediation of sectoral renewable energy consumption. *Energy Policy*, 192:114244, 2024.
- [4] Azka Amin and Eyup Dogan. The role of economic policy uncertainty in the energy-environment nexus for China: Evidence from the novel dynamic simulations method. *Journal of Environmental Management*, 292:112865, 2021.
- [5] Antony Andrews and Sean Kimpton. Econometric Forecasting of Tourist Arrivals Using Bayesian Structural Time Series. *Economic Papers*, 42(2):200–211, June 2023.
- [6] Barbara Annicchiarico, Stefano Carattini, Carolyn Fischer, and Garth Heutel. Business cycles and environmental policy: A primer. *Environmental and energy policy and the economy*, 3(1):221–253, 2022.
- [7] Mohamed Arouri, Mathieu Gomes, and Guillaume Pijourlet. Does climate policy uncertainty shape the response of stock markets to oil price changes? Evidence from GCC stock markets. *Journal of Environmental Management*, 375:124229, 2025.
- [8] Dongbei Bai, Lizhao Du, Yang Xu, and Shujaat Abbas. Climate policy uncertainty and corporate green innovation: Evidence from Chinese A-share listed industrial corporations. *Energy Economics*, 127:107020, 2023.
- [9] Zorzeta Bakaki and Thomas Bernauer. Do economic conditions affect public support for environmental policy? *Journal of Cleaner Production*, 195:66–78, 2018.
- [10] Scott R. Baker, Nicholas Bloom, and Steven J. Davis. Measuring Economic Policy Uncertainty. *The Quarterly Journal of Economics*, 131(4):1593–1636, 07 2016.

- [11] Daniel Balsalobre-Lorente, Oana M Driha, George Halkos, and Shekhar Mishra. Influence of growth and urbanization on CO₂ emissions: The moderating effect of foreign direct investment on energy use in BRICS. *Sustainable Development*, 30(1):227–240, 2022.
- [12] Emilio Barucci, Daniele Marazzina, and Aldo Nassigh. Sovereign Debt Default and Climate Risk. arXiv:2501.11552, Jan 2025.
- [13] C. Berestycki, S. Carattini, A. Dechezleprêtre, and T. Kruse. Measuring and assessing the effects of climate policy uncertainty. Technical Report 1724, OECD Economics Department Working Papers, 2022.
- [14] Rohan Best. Switching towards coal or renewable energy? The effects of financial capital on energy transitions. *Energy Economics*, 63:75–83, 2017.
- [15] Nicholas Bloom. The impact of uncertainty shocks. *Econometrica*, 77(3):623–685, May 2009.
- [16] Patrick Bolton, Lee Buchheit, Mitu Gulati, Ugo Panizza, Beatrice Mauro, and Jeromin Zettelmeyer. On Debt and Climate. *Oxford Open Economics*, 2, 07 2023.
- [17] Patrick Bolton and Marcin Kacperczyk. Global pricing of carbon-transition risk. *The Journal of Finance*, 78:3677–3754, 08 2023.
- [18] Elie Bouri, Najaf Iqbal, and Tony Klein. Climate policy uncertainty and the price dynamics of green and brown energy stocks. *Finance Research Letters*, 47, 2022.
- [19] G. E. P. Box and D. A. Pierce. Distribution of residual autocorrelations in autoregressive-integrated moving average time series models. *Journal of the American Statistical Association*, 65(332):1509–1526, 1970.
- [20] George E.P. Box, Gwilym M. Jenkins, Gregory C. Reinsel, and Greta M. Ljung. *Time Series Analysis: Forecasting and Control*. John Wiley & Sons, 2015.
- [21] Silke Bumann. What are the determinants of public support for climate policies? A review of the empirical literature. *Review of Economics*, 72(3):213–228, 2021.
- [22] Stefano Carattini, Garth Heutel, and Givi Melkadze. Climate policy, financial frictions, and transition risk. *Review of Economic Dynamics*, 51:778–794, 2023.
- [23] Andrea Carriero, Todd E Clark, and Massimiliano Marcellino. Measuring uncertainty and its impact on the economy. *Review of Economics and Statistics*, 100(5):799–815, 2018.
- [24] Tanujit Chakraborty, Donia Beshar, Madhurima Panja, and Shovon Sengupta. Neural ARFIMA model for forecasting BRIC exchange rates with long memory under oil shocks and policy uncertainties. arXiv:2509.06697, 2025.
- [25] C. Challu, Y. Kang, J. Santos, P. Montero-Manso, and R. J. Hyndman. NHITS: Neural Hierarchical Interpolation for Time Series Forecasting. arXiv:2201.12886, 2023.
- [26] Chiu-Lan Chang, Jiahui Zhang, and Yu-En Lin. Climate policy uncertainty, corporate social responsibility and corporate investments of the energy firms. *Energy Economics*, 140:107968, 2024.
- [27] Julien Chevallier. Evaluating the carbon-macroeconomy relationship: Evidence from threshold vector error-correction and markov-switching var models. *Economic Modelling*, 28(6):2634–2656, 2011.
- [28] Chulyoung Cho, Jinseok Yang, and Beakcheol Jang. Climate policy uncertainty and its impact on real estate market dynamics: A sectoral and regional analysis. *PloS One*, 19(10):e0311688, 2024.
- [29] Gamze Ozturk Danisman, Seda Bilyay-Erdogan, and Ender Demir. Economic uncertainty and climate change exposure. *Journal of Environmental Management*, 373:123760, 2025.
- [30] Eyup Dogan and Berna Turkekul. CO₂ emissions, real output, energy consumption, trade, urbanization and financial development: testing the EKC hypothesis for the USA. *Environmental Science and Pollution Research*, 23:1203–1213, 2016.
- [31] Stefan Drews and Jeroen CJM Van den Bergh. What explains public support for climate policies? A review of empirical and experimental studies. *Climate Policy*, 16(7):855–876, 2016.
- [32] J. Durbin and S. J. Koopman. A simple and efficient simulation smoother for state space time series analysis. *Biometrika*, 89(3):603–615, 2002.
- [33] Werner Ehm, Tilmann Gneiting, Alexander Jordan, and Fabian Krüger. Of quantiles and expectiles: consistent scoring functions, Choquet representations and forecast rankings. *Journal of the Royal Statistical Society Series B: Statistical Methodology*, 78(3):505–562, 2016.
- [34] J. J. Faraway. *Time Series Modeling with Applications in R*. CRC Press, 1998.
- [35] Lauren Frayer. India pledges net-zero emissions by 2070—but also wants to expand coal mining, 2021.
- [36] Brahim Gaies. Sino-American spillovers in climate policy uncertainty and financial instability: A time-varying quantile network analysis. *Journal of Environmental Management*, 386:125746, 2025.
- [37] Konstantinos Gavrilidis. Measuring Climate Policy Uncertainty, 2021. SSRN Electronic Journal.
- [38] Jiamin Ge and Boqiang Lin. Impact of public support and government’s policy on climate change in China. *Journal of Environmental Management*, 294:112983, 2021.
- [39] Francesco Giovanardi and Matthias Kaldorf. Pro-cyclical emissions, real externalities, and optimal monetary policy. *European Economic Review*, 179:105124, 2025.
- [40] C. W. J. Granger and R. Joyeux. An introduction to long-memory time series models and fractional differencing. *Journal of Time Series Analysis*, 1(1):15–29, 1980.
- [41] Clive W J Granger. Investigating causal relations by econometric models and cross-spectral methods. *Econometrica*, 37(3):424–438, July 1969.
- [42] Aslak Grinsted, John C. Moore, and Svetlana Jevrejeva. Application of the cross wavelet transform and wavelet coherence to geophysical time series. *Nonlinear Processes in Geophysics*, 11(5/6):561–566, 2004.
- [43] Gene M Grossman and Alan B Krueger. Economic growth and the environment. *The Quarterly Journal of Economics*, 110(2):353–377, 1995.

- [44] George E Halkos and Epameinondas A Paizanos. The effects of fiscal policy on CO₂ emissions: Evidence from the USA. *Energy Policy*, 88:317–328, 2016.
- [45] James Hamilton. Causes and Consequences of the Oil Shock of 2007–08. *Brookings Papers on Economic Activity*, 40:215–283, 05 2009.
- [46] Garth Heutel. How should environmental policy respond to business cycles? Optimal policy under persistent productivity shocks. *Review of Economic Dynamics*, 15(2):244–264, 2012.
- [47] Garth Heutel, Kate Ricke, and Juan Moreno-Cruz. Climate engineering economics. *Annual Review of Resource Economics*, 8:99–118, 2016.
- [48] Nguyen Thi Hoa Hong, Pham Tuan Kien, Ha Gia Linh, Nguyen Vu Ha Thanh, Nguyen Le Tuan, and Phung Duc Anh. Do climate policy uncertainty and economic policy uncertainty promote firms’ green activities? Evidence from an emerging market. *Cogent Economics & Finance*, 12(1):2307460, 2024.
- [49] Qiubin Huang. Climate versus economic policy uncertainties: Opposite implications for firm investment and firm value, 01 2025. SSRN Electronic Journal.
- [50] Rob J Hyndman and George Athanasopoulos. *Forecasting: principles and practice*. OTexts, 2018.
- [51] Tobias Ide. Recession and fossil fuel dependence undermine climate policy commitments. *Environmental Research Communications*, 2(10):101002, 2020.
- [52] Òscar Jordà. Estimation and inference of impulse responses by local projections. *American Economic Review*, 95(1):161–182, 2005.
- [53] Matthew E. Kahn and Matthew J. Kotchen. Business Cycle Effects On Concern About Climate Change: The Chilling Effect Of Recession. *Climate Change Economics*, 2(03):257–273, 2011.
- [54] Benita Katarina and Gunardi Gunardi. *Optimization of Bayesian Structural Time Series (BSTS) Applications in Forecasting Stock Prices Through State Components Selection*, pages 229–248. Springer Nature Singapore, 08 2023.
- [55] John Kenny. Economic conditions and support for the prioritisation of environmental protection during the Great Recession. *Environmental Politics*, 29(6):937–958, 2020.
- [56] Hashmat Khan, Konstantinos Metaxoglou, Christopher R Knittel, and Maya Papineau. Carbon emissions and business cycles. *Journal of Macroeconomics*, 60:1–19, 2019.
- [57] Lutz Kilian. Not All Oil Price Shocks Are Alike: Disentangling Demand and Supply Shocks in the Crude Oil Market. *American Economic Review*, 99(3):1053–69, June 2009.
- [58] Htwe Ko and Chukiatt Chaiboonsri. Forecasting International Tourist Arrivals to Myanmar During Ongoing Military Coup Period: Bayesian Structural Time Series. In *Advances in Applied Macroeconomics*, pages 21–39. Springer Nature Switzerland, 2025.
- [59] A. J. Koning, P. H. Franses, M. Hibon, and H. O. Stekler. The M3 competition: Statistical tests of the results. *International Journal of Forecasting*, 21(3):397–409, 2005.
- [60] Simon Kuznets. Economic growth and income inequality. *The American Economic Review*, 45(1):1–28, 1955.
- [61] Anh H. Le. Climate change and Carbon policy: A story of optimal green macroprudential and capital flow management. *Energy Economics*, 146:108501, 05 2025.
- [62] Kai Lessmann and Matthias Kalkuhl. Climate Finance Intermediation: Interest Spread Effects in a Climate Policy Model. *Journal of the Association of Environmental and Resource Economists*, 11(1):213–251, 2024.
- [63] C. Liang, M. Umar, F. Ma, and T. L. D. Huynh. Climate policy uncertainty and world renewable energy index volatility forecasting. *Technological Forecasting & Social Change*, 182:121810, 2022.
- [64] Quanying Lu, Yuze Li, Jian Chai, and Shouyang Wang. Crude oil price analysis and forecasting: A perspective of “new triangle”. *Energy Economics*, 87:104721, 2020.
- [65] Dandan Ma, Dayong Zhang, Kun Guo, and Qiang Ji. Coupling between global climate policy uncertainty and economic policy uncertainty. *Finance Research Letters*, 69:106180, 2024.
- [66] Anna Matzner and Lea Steininger. Firms’ heterogeneous (and unintended) investment response to carbon price increases, 2024.
- [67] Michael W McCracken and Serena Ng. FRED-MD: A monthly database for macroeconomic research. *Journal of Business & Economic Statistics*, 34(4):574–589, 2016.
- [68] Andrew G. Meyer. Do economic conditions affect climate change beliefs and support for climate action? Evidence from the US in the wake of the Great Recession. *Economic Inquiry*, 60(1):64–86, January 2022.
- [69] Axel Michaelowa and Katharina Michaelowa. Do rapidly developing countries take up new responsibilities for climate change mitigation? *Climatic Change*, 133:499–510, 2015.
- [70] Joseph Victor Michalowicz, Jonathan M Nichols, and Frank Bucholtz. *Handbook of differential entropy*. CRC Press, 2013.
- [71] Matto Mildenberger and Anthony Leiserowitz. Public opinion on climate change: Is there an economy–environment tradeoff? *Environmental Politics*, 26:1–24, 05 2017.
- [72] Silvia Miranda-Agrippino and Hélène Rey. US monetary policy and the global financial cycle. *The Review of Economic Studies*, 87(6):2754–2776, 2020.
- [73] Graziano Moramarco. Financial-cycle ratios and medium-term predictions of GDP: Evidence from the United States. *International Journal of Forecasting*, 40(2):777–795, 2024.
- [74] Nader Naifar. Spillover among sovereign credit risk and the role of climate uncertainty. *Finance Research Letters*, 61:104935, 2024.
- [75] R. G. Newell, B. C. Prest, and S. E. Sexton. The GDP-temperature relationship: Implications for climate change damages. *Journal of Environmental Economics and Management*, 108:102445, 2021.
- [76] Whitney K Newey and Kenneth D West. Hypothesis testing with efficient method of moments estimation. *International*

- Economic Review*, 28(3):777–787, October 1987.
- [77] Cheong-Fatt Ng, Kwang-Jing Yii, Lin-Sea Lau, and You-How Go. Unemployment rate, clean energy, and ecological footprint in OECD countries. *Environmental Science and Pollution Research*, 30(15):42863–42872, 2023.
 - [78] Pedi Chiemen Obani and Joyeeta Gupta. The impact of economic recession on climate change: Eight trends. *Climate and Development*, 8(3):211–223, 2016.
 - [79] Anthony O’Hagan and Jonathan J. Forster. *Kendall’s Advanced Theory of Statistics: Bayesian Inference, second edition*, volume 2B. Arnold, 2004.
 - [80] B. N. Oreshkin, D. Carпов, N. Chapados, and Y. Bengio. N-BEATS: Neural Basis Expansion Analysis Time Series Forecasting. In *International Conference on Learning Representations*, 2019.
 - [81] Ziming Pei, Xuwu Chen, Xiaodong Li, Jie Liang, Anqi Lin, Shuai Li, Suhang Yang, Juan Bin, and Simin Dai. Impact of macroeconomic factors on ozone precursor emissions in China. *Journal of Cleaner Production*, 344:130974, 2022.
 - [82] Robert Pindyck. Uncertainty In Environmental Economics. *Review of Environmental Economics and Policy*, 1, 12 2007.
 - [83] Jinwen Qiu, S. Rao Jammalamadaka, and Ning Ning. Multivariate Bayesian Structural Time Series Model. *Journal of Machine Learning Research*, 19(68):1–33, 2018.
 - [84] Hossein Rad, Rand Kwong Yew Low, Joëlle Miffre, and Robert Faff. The commodity risk premium and neural networks. *Journal of Empirical Finance*, 74:101433, 2023.
 - [85] Syed Ali Raza, Komal Akram Khan, Ramzi Benkraiem, and Khaled Guesmi. The importance of climate policy uncertainty in forecasting the green, clean and sustainable financial markets volatility. *International Review of Financial Analysis*, 91:102984, 2024.
 - [86] Moritz Ruhlmann and Folke Schulz. Wavelet coherence between economic policy uncertainty and stock markets in major economies. *Applied Economics Letters*, 27(15):1243–1248, 2020.
 - [87] D. E. Rumelhart, G. E. Hinton, and R. J. Williams. *Learning internal representations by error propagation*, page 318–362. MIT Press, 1986.
 - [88] Thomas Schreiber. Measuring information transfer. *Physical Review Letters*, 85(2):461, 2000.
 - [89] S. L. Scott and H. R. Varian. Predicting the Present with Bayesian Structural Time Series. *International Journal of Mathematical Modelling and Numerical Optimisation*, 5(1-2):4–23, 2014.
 - [90] Muhammad Shahbaz, Daniel Balsalobre-Lorente, and Avik Sinha. Foreign direct Investment–CO₂ emissions nexus in Middle East and North African countries: Importance of biomass energy consumption. *Journal of Cleaner Production*, 217:603–614, 2019.
 - [91] Claude Elwood Shannon. A mathematical theory of communication. *The Bell System Technical Journal*, 27(3):379–423, 1948.
 - [92] Natalia Sobrino and Andres Monzon. The impact of the economic crisis and policy actions on GHG emissions from road transport in Spain. *Energy Policy*, 74:486–498, 2014.
 - [93] Md Reza Sultanuzzaman, Farzan Yahya, and Chien-Chiang Lee. Exploring the complex interplay of green finance, business cycles, and energy development. *Energy*, 306:132479, 2024.
 - [94] US Environmental Protection Agency. Sources of Greenhouse Gas Emissions, 2024.
 - [95] Lukas Vacha and Jozef Barunik. Co-movement of energy commodities revisited: Evidence from wavelet coherence analysis. *Energy Economics*, 34(1):241–247, 2012.
 - [96] Qiang Wang and Shasha Wang. Decoupling economic growth from carbon emissions growth in the United States: The role of research and development. *Journal of Cleaner Production*, 234:702–713, 2019.
 - [97] Junwei Wu, Cunyi Yang, and Li Chen. Examining the non-linear effects of monetary policy on carbon emissions. *Energy Economics*, 131:107206, 2024.
 - [98] Y. Xu, M. Li, W. Yan, and J. Bai. Predictability of the renewable energy market returns: The informational gains from the climate policy uncertainty. *Resources Policy*, 79:103141, 2022.
 - [99] J. Yang, D. Dong, and C. Liang. Climate policy uncertainty and the U.S. economic cycle. *Technological Forecasting & Social Change*, 202:123344, 2024.
 - [100] Imran Yousaf, Kamel Si Mohammed, Umair Bin Yousaf, and Vanessa Serret. The effect of crypto price fluctuations on crypto mining, and CO₂ emissions amid geopolitical risk. *Finance Research Letters*, 72:106551, 2025.
 - [101] Y. Zeng, L. Liu, X. Li, Y. Wei, and Y. Hong. Transformers in time series: A survey, 2023.
 - [102] Ren Jie Zhang and Asif Razzaq. Influence of economic policy uncertainty and financial development on renewable energy consumption in the BRICST region. *Renewable Energy*, 201:526–533, 2022.
 - [103] Wenwen Zhang and Yi-Bin Chiu. Do country risks influence carbon dioxide emissions? A non-linear perspective. *Energy*, 206:118048, 2020.

A. Variable Screening and Association Analysis

This section examines the relationships between both macroeconomic and financial cycle variables, as well as public attention indicators derived from Google Trends and the primary US CPU index. To identify the most relevant predictors, we apply four complementary screening methods: Transfer Entropy, Granger Causality, Cross-Correlation, and Wavelet Coherence. These techniques capture nonlinear and linear dependencies as well as time-varying and frequency-specific associations between CPU and the candidate explanatory variables. We briefly introduce each

of these screening techniques in Sections A.1-A.4, and the results are reported in Section A.5. The findings are interpreted as predictive associations rather than causal effects.

A.1. Transfer Entropy

Information entropy was first introduced by [91]. This concept is central to measuring the amount of uncertainty or information contained in a system. Within the framework of Shannon's theory, for a coupled system (X, Y) , where $P_Y(y)$ is the probability density function (pdf) of the random variable Y , and $P_{X,Y}$ is the joint pdf of X and Y , the joint entropy between X and Y is defined as:

$$H(X, Y) = - \sum_{x \in X} \sum_{y \in Y} P_{X,Y}(x, y) \log(P_{X,Y}(x, y)).$$

The conditional entropy is given by $H(Y | X) = H(X, Y) - H(X)$, and can be interpreted as the uncertainty in Y given the knowledge of a specific value of X . Transfer Entropy, introduced by [88], has been proven to be an effective tool in identifying causal relationships in nonlinear systems. It captures the directional flow of information between systems without the need for a predefined functional form of interaction. Transfer Entropy is defined as the difference between two conditional entropies:

$$TE(X \rightarrow Y | Z) = H(Y^F | Y^P, Z^P) - H(Y^F | X^P, Y^P, Z^P),$$

where Y^F is the forward time-shifted version of Y at lag Δt with respect to past values of X^P , Y^P , and Z^P . This may also be expressed as a sum of Shannon entropies:

$$TE(X \rightarrow Y) = H(Y^P, X^P) - H(Y^F, Y^P, X^P) + H(Y^F, Y^P) - H(Y^P).$$

Since Transfer Entropy is an asymmetric measure, that is, $TE(X \rightarrow Y) \neq TE(Y \rightarrow X)$, it can be used to quantify the direction of information flow between systems. The net information flow is defined as:

$$\hat{TE}_{X \rightarrow Y} = TE_{X \rightarrow Y} - TE_{Y \rightarrow X}.$$

This quantity indicates the dominant direction of information flow, with a positive value signifying that X provides more predictive information about Y than Y does about X [70].

A.2. Granger Causality

Granger causality test is widely used for analyzing predictive power between different time series. [41] defined Granger causality as the ability to predict future values of the variable Y using past values of both X and Y . In this framework, X is said to Granger-cause Y if the inclusion of past values of X improves the prediction of Y . Let X_t and Y_t be random variables at time t , and let X_t, Y_t, Z_t represent three stochastic processes. Define \hat{Y}_{t+1} as the predictor of Y at time $t+1$. We evaluate the expected value of a loss function $g(e)$, where the error is $e = \hat{Y}_{t+1} - Y_{t+1}$, for both models. Typically, the forms of g include the L_1 or L_2 norms, and the functions f_1 and f_2 minimize the expected value of the loss function:

$$\begin{aligned} R(Y_{t+1} | Y_t, Z_t) &= \mathbb{E}[g(Y_{t+1} - f_1(Y_t, Z_t))] \\ R(Y_{t+1} | X_t, Y_t, Z_t) &= \mathbb{E}[g(Y_{t+1} - f_2(X_t, Y_t, Z_t))]. \end{aligned}$$

Definition 1. X does not G-cause Y relative to the additional information Z if and only if:

$$R(Y_{t+1} | X_t, Y_t, Z_t) = R(Y_{t+1} | Y_t, Z_t).$$

The classical Granger test is implemented via vector autoregressive (VAR(p)) model, where p is the number of lagged observations:

$$Y(t) = \alpha + \sum_{\Delta t=1}^p \beta_{\Delta t} Y(t - \Delta t) + \epsilon_t,$$

$$Y(t) = \hat{\alpha} + \sum_{\Delta t=1}^p \hat{\beta}_{\Delta t} Y(t - \Delta t) + \sum_{\Delta t=1}^p \hat{\gamma}_{\Delta t} X(t - \Delta t) + \hat{\epsilon}_t,$$

By Definition 1, X does not G-cause Y if and only if the prediction errors from the restricted and unrestricted models are equal. A one-way ANOVA test can be used to assess if the residuals differ significantly. The null hypothesis H_0 asserts that $(\gamma_1, \gamma_2, \dots, \gamma_p)$ are jointly zero, rejecting H_0 indicates that X Granger-cause Y .

A.3. Cross-Correlation

Cross-correlation is a fundamental tool in time series analysis used to examine the linear relationship between two stochastic processes at different time lags. The cross-correlation function between two stationary time series X_t and Y_t is defined as:

$$\rho_{XY}(k) = \frac{\mathbb{E}[(X_{t-k} - \mu_X)(Y_t - \mu_Y)]}{\sigma_X \sigma_Y},$$

where k represents the time lag, and $\mu_X, \mu_Y, \sigma_X, \sigma_Y$ denote the means and standard deviations of X and Y , respectively. The cross-correlation function provides a quantitative measure of the strength and direction of the linear relationship between the two series at each lag k . Significant cross-correlation at nonzero lags indicates temporal synchronization or lead-lag relationships but does not imply causal direction. Cross-correlation analysis is frequently employed in econometrics and environmental sciences to explore temporal dependencies, particularly when evaluating synchronized behaviour or transmission effects between macroeconomic and environmental indicators. However, it is limited to linear dependencies and may not adequately capture nonlinear or nonstationary relationships [20].

A.4. Wavelet Coherence

Wavelet coherence is a powerful tool for examining localized correlation and phase relationships between two nonstationary time series across time and frequency domains. Unlike classical spectral approaches, wavelet coherence captures transient associations by decomposing the signals using continuous wavelet transforms. The continuous wavelet transform of a signal $X(t)$ with respect to a mother wavelet ψ is defined as:

$$W^X(a, b) = \int_{-\infty}^{\infty} X(t) \frac{1}{\sqrt{a}} \bar{\psi} \left(\frac{t-b}{a} \right) dt,$$

where a is the scale (inversely proportional to frequency), b is the translational value, and $\bar{}$ represents the operation of complex conjugation. The cross-wavelet transform between two signals $X(t)$ and $Y(t)$ is given by:

$$W^{XY}(a, b) = W^X(a, b) W^{\bar{Y}}(a, b).$$

The wavelet coherence is then defined as:

$$R^2(a, b) = \frac{|S(a^{-1} W^{XY}(a, b))|^2}{S(a^{-1} |W^X(a, b)|^2) \cdot S(a^{-1} |W^Y(a, b)|^2)},$$

where S is a smoothing operator in time and scale. The resulting measure $R^2(a, b) \in [0, 1]$ reflects the local linear correlation between X and Y at each time-scale location (a, b) [42]. Wavelet coherence is especially suitable for analyzing nonstationary and multiscale relationships in economic and environmental time series, where the interactions may vary across frequencies and evolve over time [95; 86].

A.5. Results of Association Analyses

We apply the four complementary screening approaches to assess the predictive associations between the primary CPU index and 137 macroeconomic and financial cycle variables, as well as the Google Trends indicators. Tables A.10 and A.11 summarize the results, where “Y” indicates a statistically significant association detected by the screening procedure, while “N” denotes the absence of such an association. For transparency, Fig. A.8 provides a representative example of the wavelet coherence plots resulting from this screening method. Wavelet coherence plots are interpreted by considering both time and frequency simultaneously, represented on the horizontal and vertical axes, respectively. The color intensity indicates the degree of co-movement between the two series, with warmer colors corresponding to stronger association and cooler colors to weaker association. The orientation of the arrows shows the lead-lag relationship: arrows pointing up-left or down-right indicate that the first series leads the second, whereas arrows pointing up-right or down-left show that the second series leads the first. Regions outside the cone of influence correspond to areas where the relationship is not statistically significant.

Table A.10: Summary of statistical screening results for the macroeconomic and financial cycle variables.

Variables	Description	TE	GC	CC	W
AAA	Moody’s Seasoned Aaa Corporate Bond Yield	Y	N	N	N
AAAFFM	Moody’s Aaa Corporate Bond Minus FEDFUNDS	N	N	N	N
AMDMNOx	New Orders for Durable Goods	N	N	N	Y
AMDMUOx	Unfilled Orders for Durable Goods	N	N	N	Y
ANDENOx	New Orders for Nondefense Capital Goods	N	N	N	Y
AWHMAN	New Orders for Nondefense Capital Goods	N	N	Y	Y
AWOTMAN	Average Weekly Overtime Hours : Manufacturing	N	N	N	Y
BAA	Moody’s Seasoned Baa Corporate Bond Yield	Y	N	N	Y
BAAFFM	Moody’s Baa Corporate Bond Minus FEDFUNDS	N	N	N	Y
BCI	Business Confidence Index	Y	N	Y	Y
BOGMBASE	Board of Governors Monetary Base	N	N	N	Y
BUSINVx	Total Business Inventories	Y	N	Y	Y
BUSLOANS	Commercial and Industrial Loans	N	Y	N	Y
CAPE	Cyclically Adjusted Price/Earnings ratio	Y	N	Y	Y
CAPR	Cyclically Adjusted Price/Rent ratio	Y	Y	Y	Y
CE16OV	Civilian Employment	N	N	Y	Y
CES0600000007	Average Weekly Hours: Goods-Producing	N	N	Y	Y
CES0600000008	Average Hourly Earnings: Goods-Producing	N	Y	N	Y
CES1021000001	All Employees: Mining and Logging: Mining	N	N	N	Y
CES2000000008	Average Hourly Earnings: Construction	Y	Y	N	Y
CES3000000008	Average Hourly Earnings: Manufacturing	N	N	N	Y
CLAIMSx	Initial Claims	N	Y	N	Y
CLF16OV	Civilian Labor Force Level	N	Y	N	Y
CLI	Composite Leading Indicator	N	N	Y	Y
CMRMTSPLx	Real Manufacturing and Trade Industries Sales	N	N	N	Y
COMPAPFFx	3-Month Commercial Paper Minus FEDFUNDS	N	N	Y	Y
CONSPI	Nonrevolving consumer credit to Personal Income	N	Y	N	Y
CP3Mx	3-Month AA Financial Commercial Paper Rate	N	N	Y	Y
CPIAPPSL	CPI : Apparel	N	N	N	Y
CPIAUCSL	CPI : All Items	N	N	N	Y
CPIMEDSL	CPI : Medical Care	N	N	N	Y
CPITRNSL	CPI : Transportation	N	Y	N	Y
CPIULFSL	CPI : All Items Less Food	N	N	N	Y
CRED	Credit/GDP ratio	N	Y	Y	Y
CRED_GDP	Credit/GDP ratio	Y	Y	Y	Y
CUMFNS	Manufacturing capacity utilization	N	Y	Y	Y
CUUR0000SA0L2	CPI : All items less shelter	N	N	N	Y
CUSR0000SA0L5	CPI : All items less medical care	N	N	N	Y
CUSR0000SAC	CPI: Commodities	N	N	N	Y
CUUR0000SAD	CPI: Durables	Y	N	N	Y
CUSR0000SAS	CPI: Services	N	N	N	Y
DDURRG3M086SBEA	Personal Consumption Expenditures: Durable Goods	Y	Y	N	Y

Continued on next page

Table A.10 – continued from previous page

Variables	Full Form	TE	GC	CC	W
DMANEMP	All Employees: Durable goods	N	Y	Y	Y
DNDGRG3M086SBEA	Personal Consumption Expenditures: Nondurable Goods	N	N	N	Y
DPCERA3M086SBEA	Real Personal Consumption Expenditure	Y	N	N	Y
DSERRG3M086SBEA	Personal Consumption Expenditures: Services	N	N	N	Y
DTCOLNVHFNM	Consumer Motor Vehicle Loans Outstanding	N	Y	N	Y
DTCTHFNM	Total Consumer Loans and Leases Outstanding	N	Y	N	N
EXCAUSx	Canada/US Foreign Exchange Rate	N	N	N	Y
EXJPUSx	Japan/US Foreign Exchange Rate	N	N	N	N
EXSZUSx	Switzerland/US Foreign Exchange Rate	N	N	N	Y
EXUSUKx	US/UK Foreign Exchange Rate	N	N	N	N
FEDFUNDS	Effective Federal Funds Rate	N	N	Y	Y
GS1	1-Year Treasury Rate	Y	N	Y	Y
GS5	5-Year Treasury Rate	N	N	N	Y
GS10	10-Year Treasury Rate	N	N	N	Y
HOUST	Housing Starts: Total New Privately Owned	Y	N	N	Y
HOUSTMW	Housing Starts, Midwest	N	N	Y	Y
HOUSTNE	Housing Starts, Northeast	N	Y	Y	Y
HOUSTS	Housing Starts, South	Y	Y	N	Y
HOUSTW	Housing Starts, West	Y	N	N	Y
HPI	House Price Index	Y	N	Y	Y
HWI	Help-Wanted Index for US	N	Y	Y	Y
HWIURATIO	Ratio of Help Wanted/Number of Unemployed	Y	Y	Y	Y
INDPRO	Industrial Production (IP) Index	N	Y	N	Y
INVEST	Securities in Bank Credit at All Commercial Banks	N	N	N	N
IPB51222S	IP: Residential Utilities	N	Y	N	Y
IPBUSEQ	IP: Business Equipment	N	N	N	Y
IPCONGD	IP: Consumer Goods	N	N	N	Y
IPDCONGD	IP: Durable Consumer Goods	N	N	N	Y
IPDMAT	IP: Durable Materials	N	N	N	Y
IPFINAL	IP: Final Products (Market Group)	N	N	N	Y
IPFPNSS	IP: Final Products and Nonindustrial Supplies	N	N	N	Y
IPFUELS	IP: Fuels	N	N	N	Y
IPMANSICS	IP: Manufacturing (SIC)	N	Y	N	Y
IPMAT	IP: Materials	N	Y	N	Y
IPNCONGD	IP: Nondurable Consumer Goods	N	N	N	Y
IPNMAT	IP: Nondurable Materials	Y	Y	N	Y
ISRATIOx	Total Business: Inventories to Sales Ratio	N	N	N	Y
M1SL	M1 Money Stock	N	Y	N	Y
M2REAL	Real M2 Money Stock	Y	N	Y	Y
M2SL	M2 Money Stock	N	N	N	Y
MANEMP	All Employees: Manufacturing	Y	N	Y	Y
Mortg	Household Real Mortgage Debt Growth	N	N	N	Y
Mortg/Income	Household Mortgage/Income ratio	N	Y	N	Y
NDMANEMP	All Employees: Nondurable goods	Y	N	Y	Y
NFCI	Chicago Fed national financial condition index	N	Y	N	Y
NONBORRES	Reserves Of Depository Institutions	N	N	N	Y
NONREVSL	Total Nonrevolving Credit	N	Y	N	Y
OILPRICEx	Crude Oil, spliced WTI and Cushing	N	N	N	Y
PAYEMS	All Employees: Total nonfarm	Y	N	Y	Y
PCEPI	Personal Consumption Expenditures: Chain Index	N	N	N	Y
PERMIT	New Private Housing Permits (SAAR)	Y	N	N	Y
PERMITMW	New Private Housing Permits, Midwest (SAAR)	N	N	N	Y
PERMITNE	New Private Housing Permits, Northeast (SAAR)	Y	N	Y	Y
PERMITS	New Private Housing Permits, South (SAAR)	N	N	Y	Y
PERMITW	New Private Housing Permits, West (SAAR)	N	N	N	Y
PIP/Income	Personal Interest Payments/Income ratio	Y	N	Y	Y
PPICMM	PPI: Metals and metal products:	N	N	N	Y
PRFI/GDP	Private Residential Fixed Investment/GDP ratio	N	Y	Y	Y
REALLN	Real Estate Loans at All Commercial Banks	N	N	N	Y
RETAILx	Retail and Food Services Sales	N	N	N	Y
RPI	Real Personal Income	N	Y	N	Y

Continued on next page

Table A.10 – continued from previous page

Variables	Full Form	TE	GC	CC	W
S&P.500	S&P's Common Stock Price Index: Composite	N	N	N	Y
S&P.div.yield	S&P's Composite Common Stock: Dividend Yield	N	N	N	Y
S&P.PE.ratio	S&P's Composite Common Stock: Price/Earnings Ratio	N	N	N	Y
SP500	Real S&P500 Index Growth	N	N	N	Y
SRVPRD	All Employees: Service-Providing Industries	Y	Y	Y	Y
T10YFFM	10-Year Treasury Constant Maturity Minus FEDFUNDS	N	N	Y	Y
T1YFFM	1-Year Treasury Constant Maturity Minus FEDFUNDS	Y	N	Y	Y
T5YFFM	5-Year Treasury Constant Maturity Minus FEDFUNDS	N	N	Y	Y
TB3MS	3-Month Treasury Bill Secondary Market Rate	N	N	Y	Y
TB3SMFFM	3-Month Treasury Bill Minus FEDFUNDS	Y	N	Y	Y
TB6MS	6-Month Treasury Bill Secondary Market Rate	Y	N	Y	Y
TB6SMFFM	6-Month Treasury Bill Minus FEDFUNDS	Y	N	Y	Y
TOTRESNS	Total Reserves of Depository Institutions	N	N	N	Y
UEMP15OV	Civilians Unemployed - 15 Weeks & Over	Y	Y	N	Y
UEMP15T26	Civilians Unemployed for 15-26 Weeks	Y	Y	N	Y
UEMP27OV	Civilians Unemployed for 27 Weeks & Over	N	N	N	Y
UEMP5TO14	Civilians Unemployed for 5-14 Weeks	N	Y	N	Y
UEMPLT5	Civilians Unemployed for Less than 5 Weeks	N	N	N	Y
UEMPMEAN	Average Duration of Unemployment (Weeks)	Y	Y	N	Y
UMCSENTx	Consumer Sentiment Index	Y	N	N	Y
UNRATE	Civilian Unemployment Rate	Y	Y	Y	Y
USCONS	All Employees: Construction	N	N	N	Y
USFIRE	All Employees: Financial Activities	Y	N	N	Y
USGOOD	All Employees: Goods-Producing Industries	N	N	Y	Y
USGOVT	All Employees: Government	Y	N	N	Y
USTPU	All Employees: Trade, Transportation & Utilities	Y	N	Y	Y
USTRADE	All Employees: Retail Trade	Y	N	Y	Y
USWTRADE	All Employees: Wholesale Trade	Y	N	Y	Y
VIXCLSx	CBOE Volatility Index	N	N	N	Y
W875RX1	Real Personal Income Excluding Transfer Receipts	Y	Y	N	Y
WPSFD49207	PPI by Commodity: Finished Goods series	N	Y	N	Y
WPSFD49502	PPI by Commodity: Personal Consumption Goods	N	Y	N	Y
WPSID61	PPI by Commodity Type: Processed Goods	N	N	N	Y
WPSID62	PPI by Commodity Type: Unprocessed Goods	N	N	N	Y

Note: TE = Transfer Entropy, GC = Granger Causality, CC = Cross-Correlation, W = Wavelet Coherence.

Table A.11: Summary of statistical screening results for Google Trends indicators.

Search Terms	Description	TE	GC	CC	W
Carbon Credits (Worldwide)	Tradable credits to emit CO ₂ .	Y	N	Y	N
Carbon Emissions (Worldwide)	Total release of CO ₂ into atmosphere.	Y	Y	Y	Y
Carbon Footprint (Worldwide)	Individual or firm emissions.	Y	N	Y	Y
Carbon Tax (Worldwide)	Taxes on carbon emissions.	Y	Y	Y	Y
Clean Energy (Worldwide)	Energy from renewable sources.	Y	Y	Y	Y
Climate Action (Worldwide)	Measures to mitigate climate change.	Y	Y	Y	Y
Climate News (Worldwide)	Media coverage on climate change.	Y	Y	Y	Y
Climate Policy (Worldwide)	Policies addressing climate change.	Y	Y	Y	Y
Climate Risk (Worldwide)	Negative effects from climate change.	Y	Y	Y	Y
Climate Technology (Worldwide)	Technology reducing GHG emissions.	Y	Y	Y	Y
Electric Vehicle (Worldwide)	Battery-powered vehicles.	Y	N	Y	Y
Energy Efficiency (Worldwide)	Using less energy for same results.	Y	N	Y	Y
Energy Policy (Worldwide)	Regulations on energy consumption.	Y	Y	Y	Y
Energy Transition (Worldwide)	Shift to renewable sources.	Y	Y	Y	Y
Environmental Policy (Worldwide)	Policies addressing environmental issues.	Y	N	Y	Y
Environmental Tax (Worldwide)	Taxes on harmful activities.	Y	Y	Y	Y
Global Warming Policy (Worldwide)	Policies to limit temperature rise.	Y	N	Y	Y
Green Finance (Worldwide)	Investments promoting sustainability.	Y	N	Y	Y

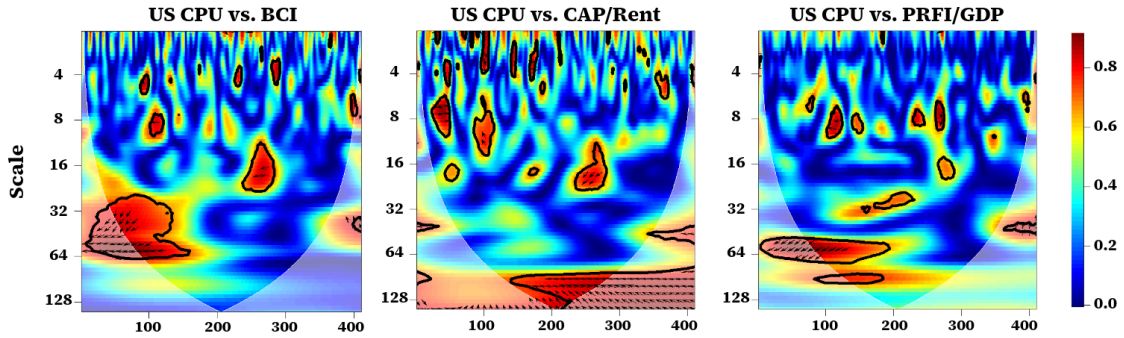
Continued on next page

Table A.11 – continued from previous page

Search Terms	Description	TE	GC	CC	W
Green Infrastructure (Worldwide)	Sustainable urban planning.	Y	Y	Y	Y
Green Jobs (Worldwide)	Employment in sustainable sectors.	Y	N	Y	Y
Green Technology (Worldwide)	Sustainable, eco-friendly technology.	Y	N	Y	Y
Greenhouse Gas Emissions (Worldwide)	Emissions of CO ₂ , CH ₄ , and N ₂ O.	Y	Y	Y	Y
Greenwashing (Worldwide)	False sustainability claims.	Y	Y	Y	Y
Renewable Energy (Worldwide)	Energy from natural sources.	Y	N	Y	Y
Sustainability (Worldwide)	Using resources wisely.	Y	Y	Y	Y
Sustainable Development (Worldwide)	Economic growth with sustainability.	Y	Y	Y	Y
Sustainable Development Goals (Worldwide)	UN-adopted framework of 17 goals.	Y	N	Y	Y
Sustainable Living (Worldwide)	Lifestyle reducing natural resources.	Y	N	Y	Y
UN Climate Conference (Worldwide)	Annual international climate summit.	Y	N	Y	Y
Zero Emissions (Worldwide)	Completely eliminating GHG emissions.	Y	Y	Y	Y

Note: TE = Transfer Entropy, GC = Granger Causality, CC = Cross-Correlation, W = Wavelet Coherence.

(a) Macroeconomic and Financial Cycle Variables



(b) Google Trends Indicators

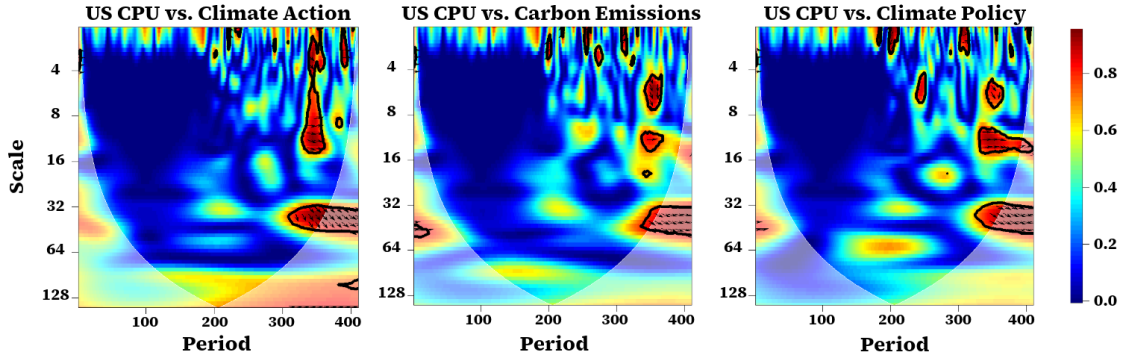


Figure A.8: Wavelet coherence plots showing time-frequency co-movement between the primary US CPU index and (a) macroeconomic and financial cycle variables and (b) Google Trends indicators. Color intensity represents the strength of association, with red indicating strong co-movement and blue weak co-movement. Arrows indicate phase relations, showing the lead-lag direction and whether series move in the same or opposite direction.

B. Components of the BSTS Model

The BSTS framework allows modeling various components to capture different features of a time series. Commonly used components include:

1. Local Level: This component models the series level as a random walk, allowing it to evolve gradually and unpredictably over time by adding small random changes at each step:

$$\mu_t = \mu_{t-1} + u_t, \quad u_t \sim \mathcal{N}(0, \sigma_u^2).$$

2. Local Linear Trend: This extends the local level by adding a slope term δ_t to account for trends that can change smoothly:

$$\mu_t = \mu_{t-1} + \delta_{t-1} + u_t, \quad \delta_t = \delta_{t-1} + v_t, \quad v_t \sim \mathcal{N}(0, \sigma_v^2).$$

3. Autoregressive Process: This component introduces an autoregressive structure of order p , denoted $\text{AR}(p)$, for some positive integer p . In an $\text{AR}(p)$ process, the current state depends on its previous p lagged observations:

$$\mu_t = \sum_{i=1}^p \phi_i \mu_{t-i} + \tilde{u}_t, \quad \tilde{u}_t \sim \mathcal{N}(0, \sigma_{\tilde{u}}^2).$$

4. Seasonal: This component captures recurring seasonal patterns by including a seasonal effect τ_t modeled through dummy variables. The parameter S denotes the length of the seasonal cycle. The seasonal component evolves according to the equation below, which imposes the constraint that seasonal effects sum to zero over one full cycle of length S .

$$\tau_t = - \sum_{s=1}^{S-1} \tau_{t-s} + w_t, \quad w_t \sim \mathcal{N}(0, \sigma_w^2).$$

5. Regression: This component allows the model to include external covariates x_t with coefficients β . The model employs a spike-and-slab prior to select relevant predictors by shrinking the coefficients of irrelevant variables toward zero with high probability. The full observation equation is:

$$y_t = \mu_t + \tau_t + \beta^\top x_t + \epsilon_t,$$

where $\epsilon_t \sim \mathcal{N}(0, \sigma^2)$ is the observation noise.

By combining these components, the BSTS model can flexibly capture a wide range of patterns, including gradual shifts, periodic fluctuations, and the influence of external covariates, found in macroeconomic time series.

C. Empirical Setup and Results

In this section, we introduce the baseline models and report the forecasting results for the alternative US CPU index and the Global CPU index.

C.1. Baseline Models

The performance of the BSTS model was evaluated against several statistical, machine learning, and deep learning models. The comparison was conducted using the following competitive frameworks:

- *Autoregressive Integrated Moving Average with exogenous variables* (ARIMA-X) model captures linear dependencies by integrating: an autoregressive (AR) component, differencing (I), and a moving average (MA) component [19]. In this framework, initially, differencing of order d is applied to obtain a stationary series. Then, the AR component models p -lagged values of the series, while the MA component models q -lagged residuals. The coefficients are estimated by minimizing the Akaike Information Criterion (AIC).
- *Autoregressive Fractionally Integrated Moving Average with exogenous variables* (ARFIMA-X) model extends the traditional ARIMA model by allowing the differencing parameter d to range between $(0, 0.5)$, enabling ARFIMA(p, d, q) to effectively handle time series exhibiting long-range dependencies, where correlations decay slowly over time [40].

- *Autoregressive Neural Network with exogenous variables* (ARNN-X) model generalizes the feed-forward neural network structure to handle autoregressive time series processes [34]. In the ARNN(p, k) model, p -lagged values are fed into the input layer and processed by k neurons in the hidden layer. Commonly, k is set to $\lfloor \frac{p+1}{2} \rfloor$. The model is first initialized with random values and trained using the gradient descent back-propagation algorithm [87]; thus achieving robust learning and preventing overfitting [50].
- *Neural Basis Expansion Analysis for Time Series with exogenous variables* (NBeats-X) framework consists of multiple blocks, each comprised of two main layers [80]. The first layer captures and models the general patterns in the data, while the second layer refines the forecasts obtained from the first layer by re-modeling the residuals. This iterative approach improves the overall forecasting accuracy.
- *Neural Hierarchical Interpolation for Time Series with exogenous variables* (NHiTS-X) is an extension of the NBeats framework by imposing a hierarchical structure. Similar to NBeats, NHiTS consists of a sequence of blocks, albeit with a hierarchical design to better capture complex dependencies and relationships in the data [25].
- *Decomposition-based Linear model with exogenous variables* (DLinear-X) decomposes the input time series into trend and seasonal components via moving average. Each component then goes through an independent linear layer, and the sum of their results is the final forecast. This method provides better performance by dealing with the trends in the data [101].
- *Normalization-based Linear model with exogenous variables* (NLinear-X) normalizes the input time series by subtracting its last value before passing it through a linear layer; then, the processed output has the subtracted value added back to produce the final forecast. This normalization technique is specially devised to cope with distribution shifts between the training and testing datasets [101].

C.2. Empirical Results

We report the forecast performance evaluation for the alternative US and Global CPU indices. Tables C.12 and C.13 present the results for the alternative US CPU index using covariate sets X_{MG} and X_M , respectively, while Tables C.14 and C.15 show the corresponding results for the Global CPU index.

Table C.12: Evaluation of the BSTS- X_{MG} model’s performance relative to baselines across all forecast horizons for the alternative US CPU index using macro-financial variables and Google Trends indicators. The **best** and **second-best** results are highlighted.

Horizon	Metric	ARFIMA- X_{MG}	ARIMA- X_{MG}	ARNN- X_{MG}	BSTS- X_{MG}	NBEATS- X_{MG}	NHiTS- X_{MG}	DLinear- X_{MG}	NLinear- X_{MG}
$h = 3$	MAPE	28.235	<u>25.453</u>	74.700	23.856	72.552	84.706	265.132	112.003
	SMAPE	24.002	21.532	47.242	<u>22.791</u>	43.399	69.297	102.337	64.737
	MAE	0.456	0.405	1.201	<u>0.428</u>	1.111	1.566	4.509	1.975
	MASE	0.909	0.808	2.393	<u>0.854</u>	2.214	3.121	8.985	3.937
	RMSE	0.540	<u>0.482</u>	1.409	0.435	1.444	1.579	4.879	2.225
$h = 6$	MAPE	25.224	20.882	61.151	<u>23.627</u>	57.011	53.303	115.042	118.338
	SMAPE	21.620	18.663	40.595	<u>23.954</u>	38.642	38.822	84.015	71.313
	MAE	<u>0.439</u>	0.375	1.046	0.469	1.078	0.978	2.568	2.422
	MASE	0.833	<u>0.711</u>	1.983	0.890	2.043	1.855	4.869	4.593
	RMSE	0.519	<u>0.472</u>	1.278	0.506	1.350	1.157	3.003	2.650
$h = 12$	MAPE	<u>36.754</u>	39.545	27.542	43.469	71.258	157.623	101.858	175.098
	SMAPE	39.351	<u>29.447</u>	22.865	44.755	50.696	78.230	71.477	134.382
	MAE	0.789	<u>0.664</u>	0.488	0.928	1.328	2.973	1.920	3.258
	MASE	1.040	0.876	<u>0.643</u>	1.224	1.751	3.920	2.532	4.295
	RMSE	0.892	0.815	<u>0.615</u>	1.140	1.500	3.309	2.314	3.652
$h = 24$	MAPE	41.518	<u>35.040</u>	55.712	33.092	57.145	58.213	99.903	95.327
	SMAPE	56.688	<u>43.424</u>	80.431	36.085	48.827	58.919	92.512	81.235
	MAE	1.411	<u>1.193</u>	1.708	<u>1.028</u>	1.399	1.637	2.321	2.465
	MASE	1.158	0.980	1.402	<u>0.844</u>	1.149	1.345	1.906	2.024
	RMSE	1.841	1.613	2.094	<u>1.416</u>	1.749	2.104	2.830	3.095

Table C.13: Evaluation of the BSTS- X_M model's performance relative to baselines across all forecast horizons for the alternative CPU index using macro-financial variables. The **best** and **second-best** results are highlighted.

Horizon	Metric	ARFIMA- X_M	ARIMA- X_M	ARNN- X_M	BSTSX $_M$	NBEATS- X_M	NHiTS- X_M	DLinear- X_M	NLinear- X_M
$h = 3$	MAPE	25.805	38.530	35.742	23.604	47.997	59.063	57.061	19.440
	SMAPE	22.204	28.426	26.582	21.697	33.872	40.144	51.832	22.104
	MAE	0.419	0.609	0.547	0.407	0.758	0.959	1.231	0.407
	MASE	0.834	1.214	1.090	0.810	1.510	1.911	2.452	0.810
	RMSE	0.480	0.780	0.707	0.428	0.935	1.138	1.467	0.475
$h = 6$	MAPE	20.882	33.645	36.804	30.750	51.802	56.481	98.123	36.783
	SMAPE	18.663	26.258	27.662	32.924	38.965	53.797	122.830	52.845
	MAE	0.375	0.581	0.620	0.630	1.024	1.018	2.004	0.721
	MASE	0.711	1.103	1.176	1.195	1.942	1.930	3.800	1.368
	RMSE	0.472	0.726	0.772	0.689	1.158	1.099	2.123	0.895
$h = 12$	MAPE	27.542	46.815	39.933	47.786	76.817	63.965	128.603	94.270
	SMAPE	22.865	59.220	47.322	34.600	51.799	41.271	102.699	86.979
	MAE	0.488	1.064	0.886	0.820	1.434	1.124	2.546	1.740
	MASE	0.643	1.403	1.168	1.081	1.890	1.482	3.357	2.295
	RMSE	0.615	1.276	1.128	0.964	1.579	1.444	3.241	2.185
$h = 24$	MAPE	35.036	46.852	39.040	34.378	49.729	89.399	112.513	111.024
	SMAPE	43.120	60.537	48.452	41.070	45.857	59.336	115.905	76.336
	MAE	1.186	1.430	1.224	1.141	1.331	1.975	2.922	2.629
	MASE	0.974	1.174	1.005	0.937	1.093	1.622	2.400	2.159
	RMSE	1.602	1.788	1.606	1.538	1.667	2.472	3.379	3.231

Table C.14: Evaluation of the BSTS- X_{MG} model's performance relative to baselines across all forecast horizons for the Global CPU index using macro-financial variables and Google Trends indicators. The **best** and **second-best** results are highlighted.

Horizon	Metric	ARFIMA	ARIMA	ARNN- X_{MG}	BSTX- X_{MG}	NBEATS- X_{MG}	NHiTS- X_{MG}	DLinear- X_{MG}	NLinear- X_{MG}
$h = 3$	MAPE	21.678	25.523	21.820	18.107	72.636	47.077	60.955	44.037
	SMAPE	19.034	22.124	19.362	16.070	53.041	37.497	46.696	35.986
	MAE	31.623	37.576	32.322	26.115	111.029	70.564	94.070	67.680
	MASE	1.223	1.454	1.250	1.010	4.295	2.730	3.639	2.618
	RMSE	35.179	40.432	34.128	30.484	111.430	72.594	94.266	68.074
$h = 6$	MAPE	16.361	16.517	16.314	16.176	49.647	34.694	40.944	39.588
	SMAPE	18.174	17.444	17.251	16.179	38.604	29.221	32.472	32.322
	MAE	32.047	30.796	30.499	28.673	84.072	57.717	67.496	65.293
	MASE	1.145	1.100	1.090	1.024	3.004	2.062	2.411	2.333
	RMSE	38.664	34.548	34.421	32.601	88.740	62.155	74.414	74.278
$h = 12$	MAPE	12.979	16.409	11.397	15.553	73.687	43.982	40.884	39.604
	SMAPE	13.921	15.176	12.371	14.596	51.559	34.386	31.838	30.210
	MAE	23.595	26.080	21.095	25.012	116.900	69.070	64.398	62.770
	MASE	1.114	1.231	0.996	1.181	5.518	3.260	3.040	2.963
	RMSE	32.527	29.357	28.467	28.018	125.711	77.471	75.484	78.708
$h = 24$	MAPE	29.670	22.647	23.918	18.247	33.289	31.992	41.402	34.669
	SMAPE	35.654	26.065	27.752	20.305	29.736	28.029	40.439	34.690
	MAE	56.315	43.536	45.537	35.001	54.837	52.483	71.323	60.076
	MASE	1.464	1.132	1.184	0.910	1.426	1.365	1.854	1.562
	RMSE	64.629	53.344	53.903	44.656	62.984	61.232	85.001	70.294

Table C.15: Evaluation of the BSTS- X_M model's performance relative to baselines across all forecast horizons for the Global CPU index using macro-financial variables. The **best** and *second-best* results are highlighted.

Horizon	Metric	ARFIMA	ARIMA	ARNN- X_M	BSTSX $_M$	NBEATS- X_M	NHiTS- X_M	DLinear- X_M	NLinear- X_M
$h = 3$	MAPE	21.678	25.523	<i>11.617</i>	21.721	56.689	54.437	30.964	10.193
	SMAPE	19.034	22.124	10.850	19.153	43.734	42.673	26.419	9.281
	MAE	31.623	37.576	<i>17.083</i>	31.879	86.300	83.537	46.226	14.717
	MASE	1.223	1.454	0.661	1.233	3.338	3.231	1.788	0.569
	RMSE	35.179	40.432	18.467	34.705	87.543	83.834	47.823	19.896
$h = 6$	MAPE	16.361	16.517	14.931	<i>16.357</i>	43.532	28.335	15.792	23.141
	SMAPE	18.174	17.444	<i>16.544</i>	17.353	34.591	26.207	15.226	27.960
	MAE	32.047	30.796	<i>29.458</i>	30.643	72.948	48.570	26.854	46.196
	MASE	1.145	1.100	<i>1.052</i>	1.095	2.606	1.735	0.959	1.650
	RMSE	38.664	34.548	35.911	<i>34.564</i>	78.107	54.100	35.289	58.055
$h = 12$	MAPE	12.979	16.409	18.982	<i>15.442</i>	87.385	47.419	30.174	17.991
	SMAPE	13.921	15.176	21.546	<i>14.499</i>	58.467	37.072	25.068	19.554
	MAE	23.595	26.080	33.537	<i>24.837</i>	139.414	75.537	47.434	31.696
	MASE	1.114	1.231	1.583	<i>1.172</i>	6.581	3.566	2.239	1.496
	RMSE	32.527	<i>29.357</i>	39.140	27.913	147.778	81.757	55.299	40.667
$h = 24$	MAPE	29.670	<i>22.647</i>	35.113	18.286	30.848	30.722	31.056	31.936
	SMAPE	35.654	26.065	44.348	20.402	32.174	29.215	29.843	38.486
	MAE	56.315	<i>43.536</i>	64.709	35.155	55.289	52.665	53.416	60.074
	MASE	1.464	<i>1.132</i>	1.682	0.914	1.438	1.369	1.389	1.562
	RMSE	64.629	<i>53.344</i>	72.359	44.900	66.888	60.151	65.973	75.612